UNIVERSITY OF ÇUKUROVA
INSTITUTE OF NATURAL AND
APPLIED SCIENCES

MSc THESIS

SUAT SARI

VARIABLE FREQUENCY CONTROL OF INDUCTION MOTORS

DEPARTMENT OF ELECTRICAL AND
ELECTRONICS ENGINEERING

ADANA, 2002

ÇUKUROVA ÜNİVERSİTESİ
FEN BİLİMLERİ ENSTİTÜSÜ

VARIABLE FREQUENCY CONTROL OF INDUCTION MOTORS

SUAT SARI
YÜKSEK LİSANS TEZİ
ELEKTRİK-ELEKTRONİK MÜHENDİSLİĞİ ANA BİLİM DALI

Bu tez 10.08.2002 Tarihinde Aşağıdaki Jüri Üyeleri Tarafından Oybirliği/Oyçokluğu ile Kabul Edilmiştir.

İmza................	İmza................	İmza................
Prof.Dr.Julian RICHARDSON	Prof. Dr.A. Hamit SERBEST	Doç. Dr. Mehmet TÜMAY
DANIŞMAN	ÜYE	ÜYE

Bu tez Enstitümüz Elektrik-Elektronik Mühendisliği Anabilim Dalında hazırlanmıştır.

Kod No: 2052

Prof.Dr. Fikri AKDENİZ
Enstitü Müdürü

ABSTRACT

MS THESIS

VARIABLE FREQUENCY CONTROL OF INDUCTION MOTORS

Suat SARI

DEPARTMENT OF ELECTRICAL AND ELECTRONICS ENGINEERING
INSTITUTE OF NATURAL AND APPLIED SCIENCES
UNIVERSITY OF ÇUKUROVA

Supervisor : Prof.. Dr. Julian RICHARDSON
Year:2002 Pages: 79

Jury : Prof.. Dr. Julian RICHARDSON
Prof. Dr. A. Hamit SERBEST
Assoc. Prof. Dr. Mehmet TÜMAY

Variable frequency control of induction motors requires careful analysis for a number of different operational conditions. An induction motor is generally designed for operation on one specific voltage and frequency supply. A variable voltage and frequency supply enables speed control of the motor over a wider range compared to other methods such as voltage or rotor resistance control. It is important that the flux density in the magnetic system is kept at an acceptable level over the range of speeds required. This necessitates a voltage supply whose voltage is approximately proportional to the frequency.

The performance of an induction motor over its useful speed range and also its performance at the lower and higher ends of that range is investigated. The current accepted range for a 50 Hz is verified and evaluated as from 10 to 100 Hz, with deteriorated performance at the ends of this range. The particular voltage/frequency source is by Pulse Width Modulation (PWM) control.

Keywords: PWM, speed control of induction motors,

ÖZ

YÜKSEK LİSANS TEZİ

ENDÜKSİYON MOTORLARIN DEĞİŞKEN FREKANS KONTROLU

Suat SARI

ÇUKUROVA ÜNİVERSİTESİ
FEN BİLİMLERİ ENSTİTÜSÜ
ELEKTRİK-ELEKTRONİK MÜHENDİSLİĞİ ANA BİLİM DALI

Danışman : Prof.. Dr. Julian RICHARDSON
Yıl:2002 Sayfa: 79

Jüri : Prof.. Dr. Julian RICHARDSON
Prof. Dr. A. Hamit SERBEST
Doç. Dr. Mehmet TÜMAY

Bir endüksiyon motoru genellikle çalışmaları için belirli bir voltaj veya frekansa göre tasarlanırlar. Değişken voltaj ve frekans sağlayıcılar motorun hız kontrolünü voltaj veya rotor rezistans kontrol metotlarına oranla daha geniş bir alanda mümkün kılar. Manyetik sistemdeki akış yoğunluğunu istenilen hızların bölgesi üzerinde kabul edilebilir bir seviyede devam ettirebilmek önemlidir. Bu voltajı frekansa orantılı bir voltaj kaynağını gerekli kılar.

Bu projede bir endüksiyon motorun 50 Hz olan çalışma frekansı ile ayrıca sistemin müsaade ettiği mümkün olan bu alanın daha düşük ve yüksek uçlarındaki 10 Hz ve 100 Hz deki performansı araştırıldı. Değişken voltaj/frekans kaynağı olarak PWM (Pulse Width Modulation) kontrole sahip bir kaynak kullanıldı.

Anahtar Kelimeler: PWM, İndüksiyon motorların hız kontrolü

ACKNOWLEDGEMENTS

I would like to express my gratitude to my supervisor Prof. Dr. Julian RICHARDSON for his support, guidance, suggestions and encouragements.

I would like to express my appreciation to Prof. Dr. A. Hamit SERBEST and to Chairman of the Department of Electrical and Electronics Engineering, Prof. Dr. Süleyman GÜNGÖR for their support.

I would like to thank to my son Alper , my wife Rukiye and my parents for their help, moral support and especially tolerance.

CONTENTS PAGE

LIST OF SYMBOLS

PWM	Pulsewidth Modulation
f_r	Frequency ratio
N_s	Synchronous speed
f	Frequency
P	Pairs of poles
N_r	Actual rotor speed
V_m	counter emf
R_m	Equivalent resistance for excitation loss
L_m	Magnetizing inductance
R_s	Stator resistance
R_r	Rotor resistance
w_{sl}	Rotor slip frequency
I_s	Stator current
I_r	Rotor current
T_e	Developed torque
w_e	Stator electrical speed
w_r	Rotor mechanical speed
Vn	nth harmonic amplitude component normalized to the DC supply where n is the order of the particular harmonic (i.e., n = 1,3,5,7........)
α_i	i^{th} switching angle in relation to the PWM frequency, where i = 1,3,5,7........k, and k is the selected number of switching angle Per quarter cycle of the PWM waveform.
V/f= *constant*	Torque profile criterion for induction motors

LIST OF FIGURES

1. INTRODUCTION

The three-phase Cage Rotor Induction Motor is probably the most frequently used of all electrical drives, especially in industrial applications. These machines are very popular because of combination of its relatively low cost, robust construction, compact size, reliability and minimal servicing and maintenance requirement. Normally, pure AC supply is necessary to operate an induction motor, but AC drives can be used with controlled voltage and frequency supplies. Although there are a lot of ways to provide variable voltage-variable frequency waveforms for AC machines, one of the most favored of them is by the process of Pulse Width Modulation (PWM). PWM provides voltage and frequency control and means of adjusting the harmonic content of the waveform by altering a single parameter which is the frequency ratio f_r.

Recent development and advances in power electronics and, as parallel to this development, drive control technology, have made AC machines better alternatives to the DC machine to operate efficiently at variable speeds for performing the same task. This is seen in many areas such as drives for fans, pumps, conveyors, mixers, elevators etc.

1.1. Review of AC Drives and Speed Control Methods

AC drives, inverters, and adjustable frequency drives(or adjustable speed drives-ASD) are all terms that are used to refer to equipment designed to control the speed of an AC motor. AC drives receive AC power and convert it to an adjustable frequency, adjustable voltage output for controlling motor operation..

ASDs normally take a 50 Hz or 60 Hz AC input and generate a variable frequency output to control the speed of the motor as necessary to meet the load demand. Figure 1.1 shows a simplified layout of an ASD. The rectifier converts the incoming AC power to a DC output. The DC link further reduces any ripple in the rectifier output.

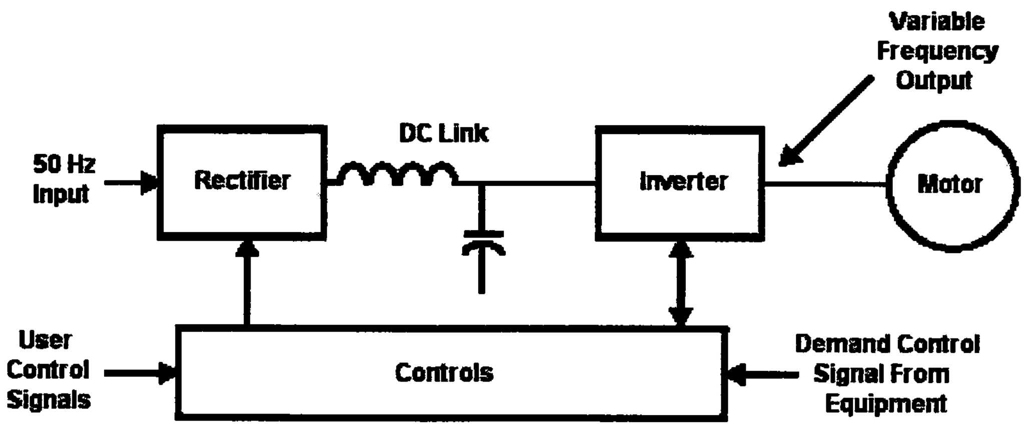

Figure 1.1 Simplified layout of an Adjustable Speed Drive.(Conkling,2000)

The inverter circuit converts its dc input into a variable frequency ac voltage to control the speed of an induction motor.

The torque/slip characteristic shown in Figure 2.2 is typical for a three-phase cage rotor induction motor supplied from a conventional constant voltage and constant frequency AC mains supply.

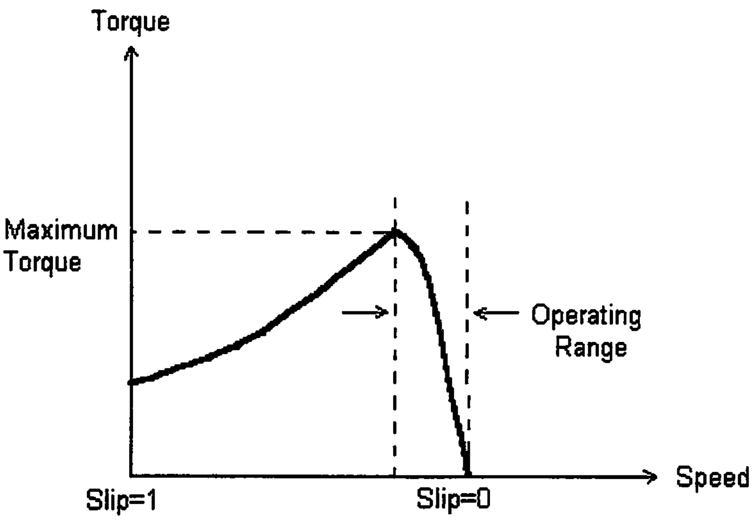

Figure 1.2 Torque/speed curve of an cage rotor induction motor

Although on no-load the rotor slip is theoretically zero, in practice this is not normally achievable because of mechanical and electrical losses. This is detailed in the next section. As the load is increased the speed of the motor reduces until the condition is reached where the maximum torque of machine is being produced. The nominal speed of an induction motor is governed by the design of the stator field windings and also by the supply frequency. For a machine with P pairs of poles per phase and supplied frequency of f, the nominal (synchronous) speed is given by the equation,

$$N_s = \frac{60\,f}{P} \quad rpm. \tag{1.1}$$

The difference between the synchronous speed of the induction motor and the actual rotor speed is termed the slip (s) of the motor. This can be expressed as,

$$slip = \frac{N_s - N_r}{N_s} \tag{1.2}$$

slip may be also expressed as proportion or percentage of synchronous speed.

$$slip = \frac{N_s - N_r}{N_s}\, x\, 100\,\% \tag{1.3}$$

It can be seen from the above equations that the speed of an induction motor may be varied by changing number poles. The stator of a cage rotor induction motor consist of three-phase circuit designed to produce a rotating magnetic field when connected to a three-phase supply. In general, it is only possible to wind a magnet with an even number of poles, a North/South pole pair. So, the stator can only have even number of poles such as 2, 4, 6, 8 etc. This would produce synchronous speed of 3000, 1500, 1000, 750 rpm respectively, when used with a 50 Hz supply. Hence the disadvantage of this method of speed control is that the speed range is not infinitely variable and has to be pre selected at the time of specification and only step changes in speed are possible.

It can be seen from equation (1.1) that the synchronous speed of an induction motor can be chanced by varying the supply frequency to the stator windings and synchronous speed of motor will vary in direct proportion. So, with a power supply of infinitely variable output frequency by using an inverter/motor system, the motor speed may be adjusted to the exact speed value required.

If an induction motor is to be used at supply frequencies other then the value for which is designed, other operation factors have to be taken into consideration. One of the most important of them is the impedance of stator winding which varies with supply frequency, is due to the winding's inductive reactance. Increasing the supply frequency, increases the winding impedance and at constant voltage this would result in a reduction of current and lead to a loss of potential mechanical output and also cause saturation of the magnetic circuit, overheating of the windings and possible damage to the actual windings themselves.

Decreasing the supply frequency, reduces the winding impedance. At constant voltage, this would result in an increase in stator current. Variation in current is overcame by maintaining the voltage to frequency ratio constant:

$$\frac{Voltage\,(V)}{Frequency\,(f)} = Constant \qquad (1.4)$$

At low speeds, however, the reduced voltage limits the current and consequently reduces the induction motor's starting capabilities, especially against an applied load and in practice to overcome this poor low speed performance, it is common to incorporate a voltage boost facility into the variable frequency drive.

Another speed control method is slip power recovery control and this system using static Kramer method is shown in figure 1.3.

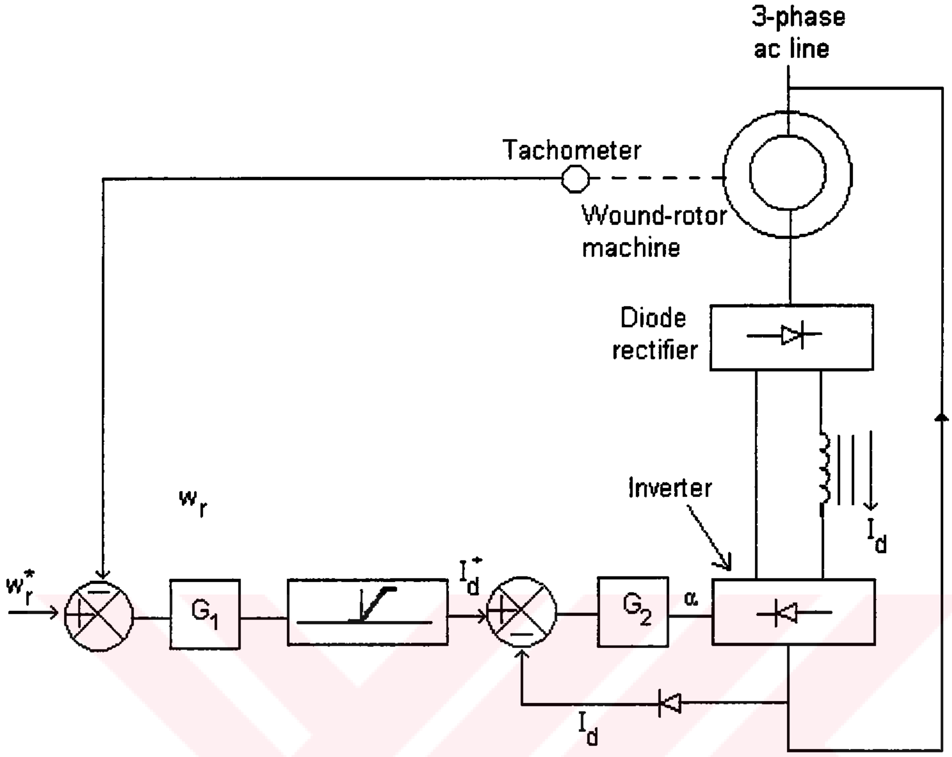

Figure 1.3 Speed control of static Kramer drive system. (Bose,1986(a))

With a constant air gap flux, the torque is proportional to dc link current I_d, which is controlled by a feedback loop. Instead of sensing I_d directly, 50 or 60 Hz line current is sensed by current transformers and rectified to get the I_d signal. The speed control loop added over the current control loop , as shown. The control is fairly simple but a disadvantage is that the drive system can be controlled in one quadrant only. If the command speed is increased by a step, the motor accelerates at constant developed torque corresponding to the I_d^* limit set by the speed control loop. As the actual speed approaches the command speed, the dc link current is reduced so as to balance with the load torque. If the speed command is decreased by a step, I_d approaches zero and machine slows down with load torque. Then as the speed error tends to be zero in steady state, I_d is restored to balance with load torque. The air gap flux remains approximately constant during the whole operation, as dictated by the stator voltage and frequency. With a finite load torque, the rotor speed is always less than the synchronous speed. For motoring operation at true synchronous speed, the rotor requires dc excitation current. The dc power can be supplied by operating the inverter as a rectifier, but the inverse polarity of dc link voltage will short circuit the diode rectifier, bypassing the rotor winding.

Although the cage type induction motor is most commonly used in wide power range, wound-rotor machines with slip power recovery control (known as static Kramer and Scherbius drives) have been generally used in limited speed range multi-megawatt drive applications, because of expensive machine costs and poor system performance, as suggested by(Bose,2000(c))

Another two speed control methods are changing the line voltage and rotor resistance. First one is detailed in the next section. The other one is changing the rotor resistance. In this method, speed can be controlled by varying the rotor circuit resistance. Additionally this method has limited constant torque region and speeds above rated speed are not possible.

1.2. Development of the Application of Power Electronics for Control of AC Drives

As the cost of power electronics is falling and the system performance is improving, its applications are having an important place in industrial, commercial, residential, utility, aerospace and military systems. Modern industrial processes, transportation and energy systems benefit tremendously in productivity and quality enhancement with the help of power electronics and today's progress in power electronics has been possible primarily due to advances in power semiconductor devices. Apart from device evolution, the inventions in converter topologies, PWM techniques, analytical and simulation methods, control and estimation techniques, computers, digital signal processors, control hardware and software, etc. have also contributed to this progress.

In looking at the historic origins of modern drives it is important to note that the inherently fixed speed, three-phase squirrel cage induction motor was introduced in 1889, and then the slip-ring induction motor a year later. The speed of these motors depends fundamentally upon pole number and supply frequency.

Historically, the power electronics age began with the invention of glass-bulb mercury-arc rectifier at the beginning of this century (1901). In 1923 the Ignitron made Controlled Rectification Possible. The Thyratron and Grid Controlled Mercury Rectifiers made life easier in 1928. This made possible the direct control of voltage applied to the Armature of a DC machine so as to apply the philosophy of Ward Leonard control without additional machines. (Drury), (Bose,2000(c))

Then, by the early 1930's the ideas of inversion (DC to variable frequency / voltage AC which is the basis for the present day inverter) had been established, the use of forced commutation by means of switched Capacitors was introduced. Direct AC to AC conversion by means of Cycloconverters was introduced in 1931 for railway service. (Drury)

However, the modern era of solid-state power electronics started with the invention of thyristor (or silicon-controlled rectifier) in the late 1950's. Gradually, other devices, such as triac, gate turn-off thyristor (GTO), bipolar power transistor (BPT or BJT), power MOSFET, insulated gate bipolar transistor (IGBT), static induction transistor (SIT), static induction thyristor (SITH), MOS-controlled thyristor (MCT), integrated gate-commutated thyristor (IGCT) and power semiconductor diode were introduced..

In the 1960's, when inverter-grade thyristors appeared, various types of voltage-fed force-commutated thyristor inverters, such as McMurray inverter, McMurray-Bedford inverter, Verhoef inverter, ac-switched inverter and dc-side commutated inverter were introduced. Many other commutation techniques are highlighted in the literature. However, many of this class of inverters gradually faced obsolescence because of the advent of self-commutated GTO's and bipolar transistors. Among the PWM techniques, sinusoidal voltage control PWM and hysteresis-band instantaneous current control PWM became very popular.

Then the advent of large Darlington BJT's in the 1970's brought great expectations in power electronics. Recently, and almost suddenly, the device has been totally ousted in competition with power MOSFET (low voltage range) and

IGBT (higher voltage). The introduction of IGBT in the 1980's was an important milestone in the history of power semiconductor devices. Its switching frequency is much higher than that of BJT, and square SOA (safe operating area) permits easy snubberless operation. The power rating (currently 3500 V, 1200 A) and electrical characteristics of the device are continuously improving. (Bose,2000(c))

In 1986, great advances were being made at this time in the field of microprocessors making possible cost effective Digital Drives. In 1986 CT introduced the first successful standard Digital DC Drive to the world market. This drive broke new ground in regard the use of Custom Integrated Circuits; which to that time had only used in exceptionally large volume/domestic applications. (Drury)

To day, the pace of change goes on. Perhaps worthy of note are the advances in Power Semiconductors and the ongoing developments in the area of Integrated Power Modules started in 1990.

Parallel to the rapid development of power semiconductors, the advent of powerful microcomputers, digital signal processors, personal computers, CAD and simulation tools, AI techniques, and advancement of control and estimation theories has continuously extended the frontier of control and estimation techniques. Although simple volts/Hz control has been known for a long time, and is extensively used in low performance industrial drives, the advent of vector or field-oriented control since the 1970s brought improvement in modern high performance control of ac drives. It has been widely accepted for applications, such as paper and textile mills, metal rolling mills, servos and machine tools, elevators, electric vehicles, etc. where dc machine-like performances are demanded. In spite of complexity, this type of control is expected to be universal for ac drives in future. Vector control can be classified into indirect and direct methods, and can be based on rotor or stator flux orientation.

A type of performance-enhanced scalar control, called direct torque and flux control (known as DTC) which was proposed in the 1980's, is receiving a lot of attention in the recent literature. The DTC control gives adequately fast response, has the simplicity of implementation due to absence of close loop current control, and traditional PWM algorithm and vector transformation. However, the inherent demerits of limited cycle operation, such as pulsating torque, pulsating flux and additional machine harmonic loss exist. Since the torque and stator flux vector are estimated from machine voltages and currents, the low speed limitation and parameter variation problem are similar to stator flux oriented vector control.

Recently, modern trends in designing numeric control systems are utilization of algorithms of fuzzy logic, and the use of artificial neural networks. The fuzzy logic is used for control of systems whose mathematical models are not known or difficult to define, and also for the control of systems of time-variable or nonlinear nature. Design and tuning procedures of fuzzy controllers do not require formulating mathematical models for the systems to be controlled, the gist of the method being in the final tuning of control parameters. Control algorithms with fuzzy logic are expected to simplify numeric control systems as well as to improve their withstanding capacity to changes of parameters. Artificial neural networks are can to be used for control of electric drives in combination with algorithms of fuzzy logic. So, better effectiveness, higher velocity of control, and also better adaptability are possible (Bose, Grabowski and Kazmierkowski, 2000), (Mihoub, Mazari and Fasla, 2001), (Mohaddes,1998).

1.3. Techniques of Variable Frequency and Voltage Generation, Cycloconverters, Inverters, PWM

In industrial applications, two forms of electrical energy are used: direct current (DC) and alternating current (AC). Usually constant voltage constant frequency single-phase or three-phase AC is readily available. However, for different applications, different (AC or DC) magnitudes and/or frequencies are required. There are four different conversions between dc and ac power sources. The converters can be classified as, rectifiers, which convert from single-phase or three-phase AC to variable voltage DC, choppers, which convert from DC to variable voltage DC, inverters, which convert from DC to variable magnitude and variable frequency, single-phase or three-phase AC and cycloconverters, which convert from single-phase or three-phase AC to variable magnitude and variable frequency, single-phase or three-phase AC.

The three common inverter types are the variable voltage inverter (VVI), current source inverter (CSI), and pulse width modulation (PWM).

The variable voltage inverter (VVI) which is shown in Figure 1.4 is sometimes called voltage source inverter (VSI) or six-step inverter. It uses an SCR converter Inverter (VVI) bridge to convert the incoming AC voltage into DC. The SCRs provide a means of controlling the value of the rectified DC voltage from 0 to approximately 600 VDC. The L1 choke and C1capacitor(s) make up the DC link section and smooth the converted DC voltage.

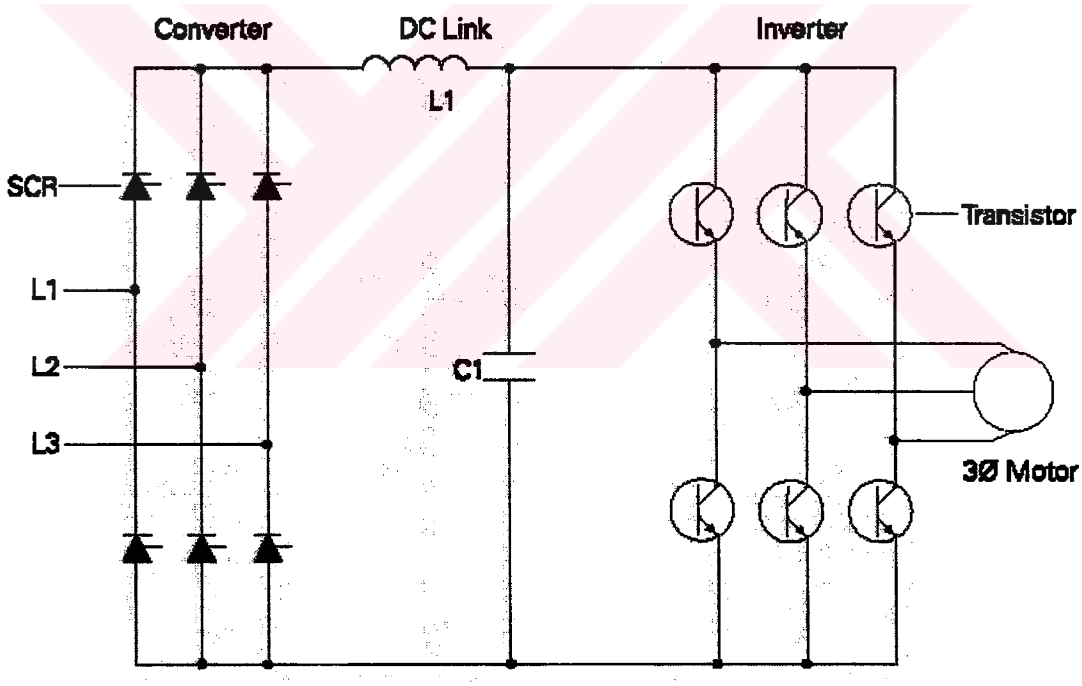

Figure 1.4 Voltage Source Inverter (Siemens)

The inverter section consists of six switching devices. Various devices can be used such as thyristors, bipolar transistors, MOSFETS, and IGBTs. Transistors and Control logic which is not shown in Figure 1.4 uses a microprocessor to switch the transistors on and off providing a variable voltage and frequency to the motor. It is used in low to medium power applications, generally up to a few hundred horsepower. Advantages include simple circuit configuration, high efficiency over a wide speed range (10 to 200 percent) and ability to control several motors at once. A main disadvantage is torque pulsation which occurs each time a switching device, such as a bipolar transistor, is switched. The pulsations can be noticeable at low speeds as speed variations in the motor. These speed variations are sometimes referred to as cogging. The non-sinusoidal current waveform which is shown in Figure 1.5 causes extra heating in the motor requiring a motor derating.

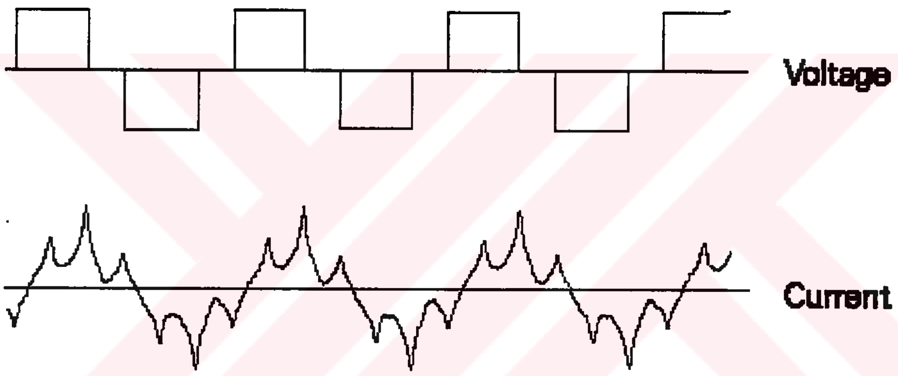

Figure 1.5 Voltage and current waveform of output of VSI(Siemens)

A CSI which is shown in Figure 1.6 actually uses the inductive characteristic of the motor to stabilize DC as it reaches the inverter. Because the inductor has to be fairly large to keep the current source stable, this type of electronic ASD is generally used with 100 hp and larger drives. It is harder to tune in use because it cannot operate without connection to the motor. Advantages of CSIs include regenerative braking capability (acting as a generator while motor is slowing down), good short-circuit protection, high efficiency at a wide range of speeds above 50 percent, quiet operation, relative ruggedness, and simplicity.

Disadvantages include poor power factor at low speed/load, potential for oscillating (reversing) torque at speeds less than 10 percent, and inability to test the drive without attaching the motor (which must be matched to the inverter).

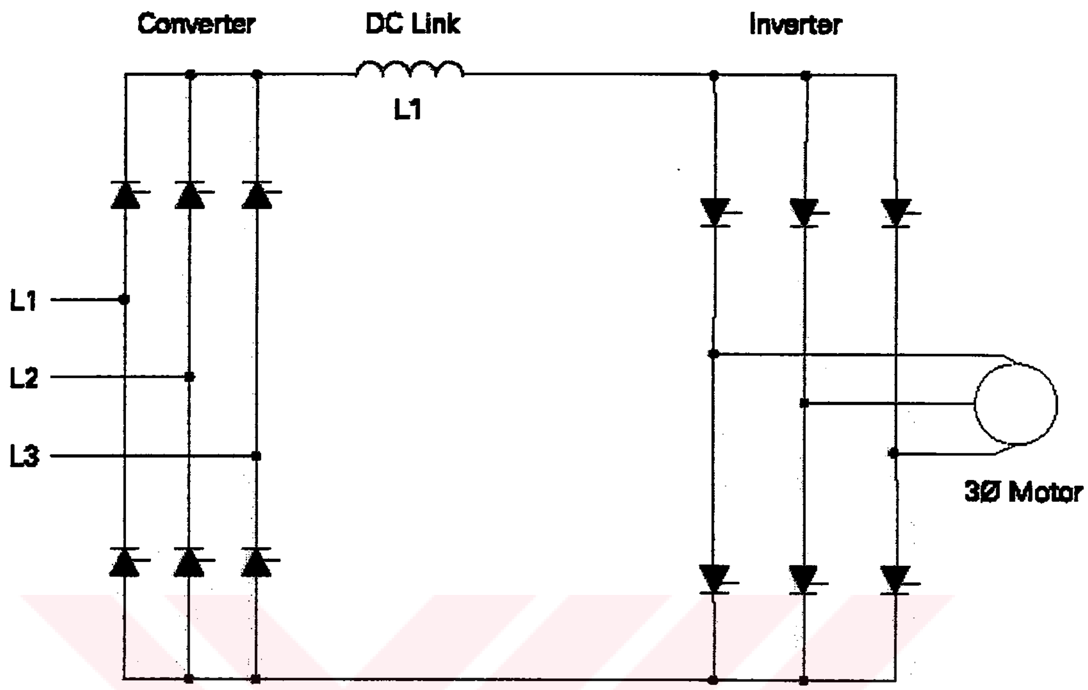

Figure 1.6 Current Source Inverter (Siemens)

This type of drive which is output waveforms shown in Figure 1.7 is usually used to drive only one motor at a time, although more than one is physically possible.

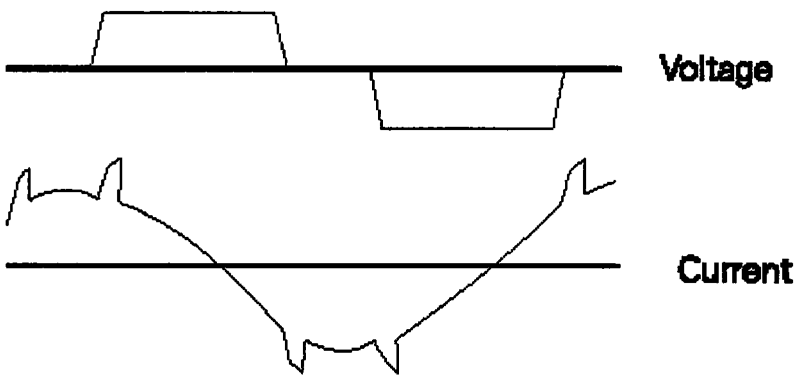

Figure 1.7 Voltage and current waveform of output of CSI (Siemens)

Pulse Width Modulation, whose complete circuit shown in Figure 1.8, is the process of the pulses in a pulse train in direct proportion to a small control signal; the greater the control voltage, the wider the resulting pulses become. By using a sinusoid of the desired frequency as the control voltage for a PWM circuit, it is possible to produce a high-power waveform whose average voltage varies sinusoidally in a manner suitable for driving ac motors.

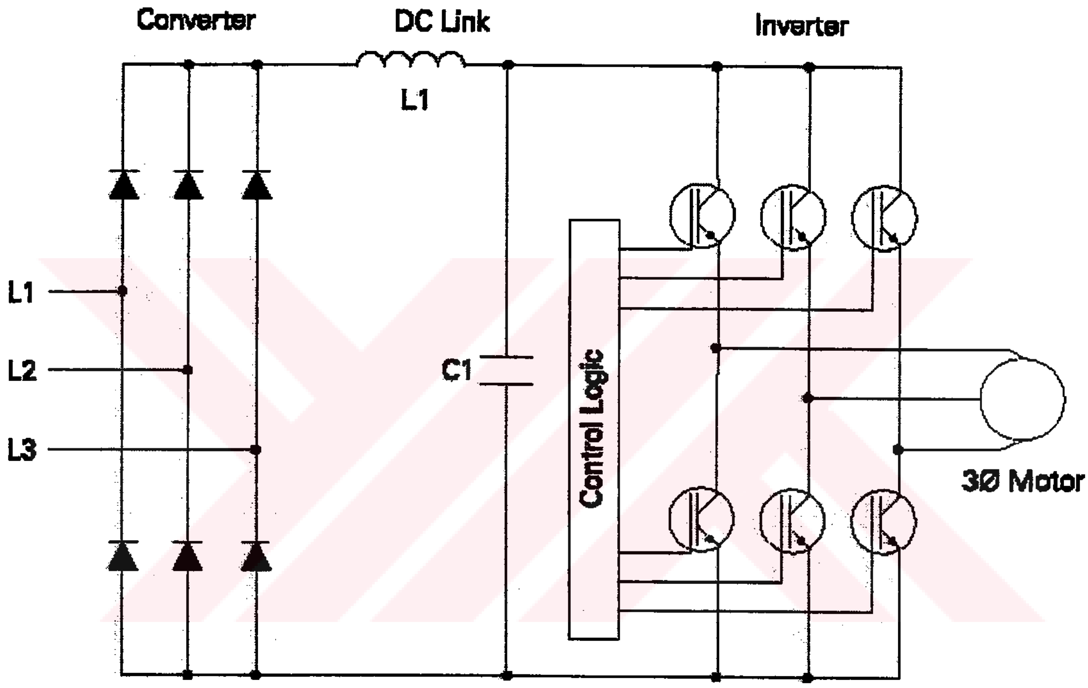

Figure 1.8 Pulse Width Modulation Inverter circuit.(Siemens)

Figure 1.9 shows the basic concept of PWM. Figure 1.9a shows a single-phase PWM inverter circuit using IGBTs. The states of IGBTs in this circuit are controlled by the two comparators which is shown in Figure 1.9b.

A comparator is device which compares the input voltage $V_{in}(t)$ to a reference signal and turns transistor on or off depending on the result of the test. Comparator A compares $V_{in}(t)$ to the reference voltage $V_x(t)$ and controls IGBTs T_1 and T_2 based on the results of comparison. Comparator B compares $V_{in}(t)$ to the reference voltage $V_y(t)$ and controls IGBTs T_3 and T_4 based on the results of comparison. If $V_{in}(t)$ is greater then $V_x(t)$ at any given time t, then comparator A will turn on T_1 and turn off

T_2. Otherwise, it will turn off T_1 and turn on T_2 and Comparator B works in the same sense. The reference voltages $V_x(t)$ and $V_y(t)$ are shown in Figure1.10

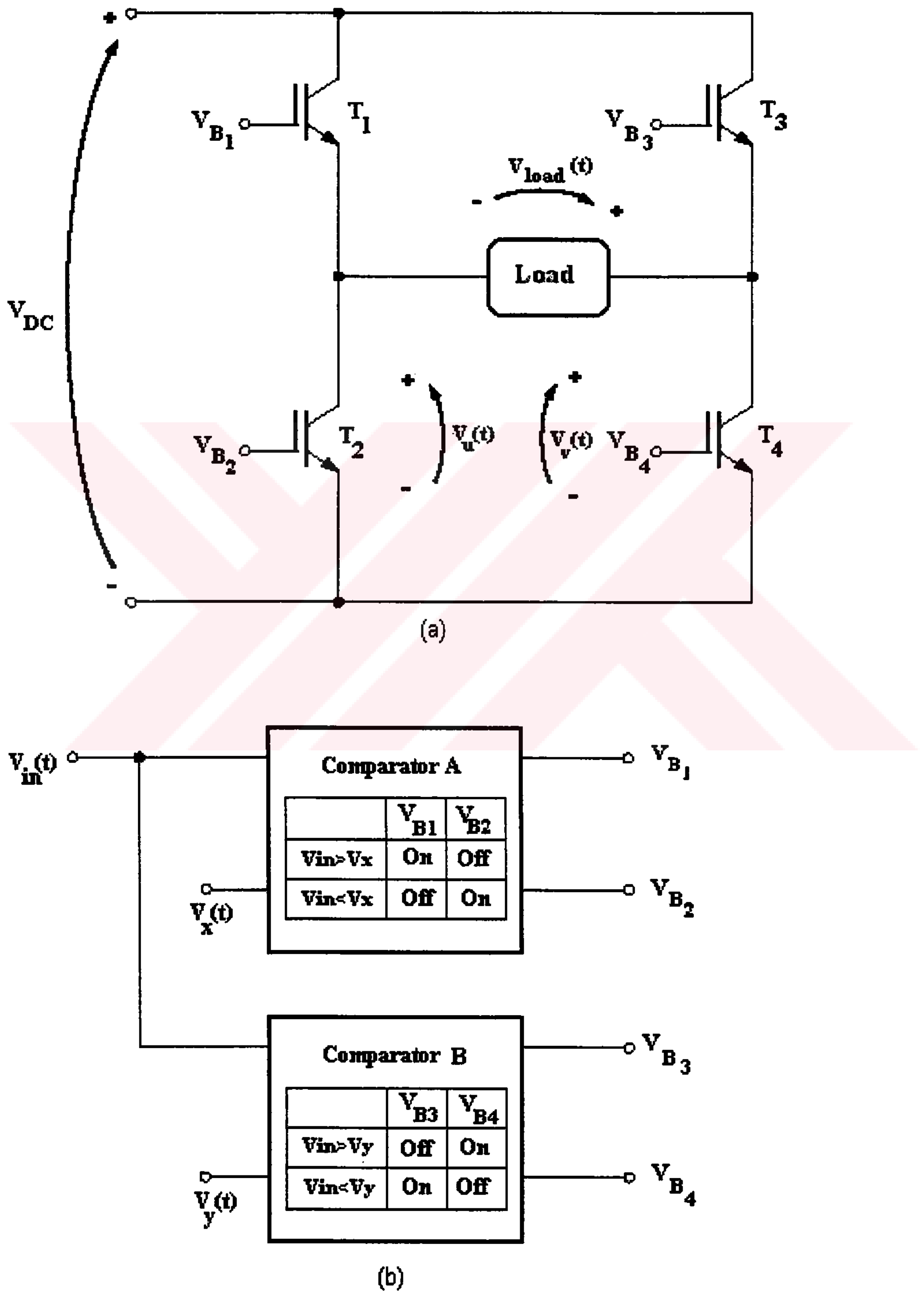

Figure 1.9 The basic concept of PWM (a) A singl-phase PWM circuit (b) The comparators used to control the on and off states of transistors.(Chapman,2002)

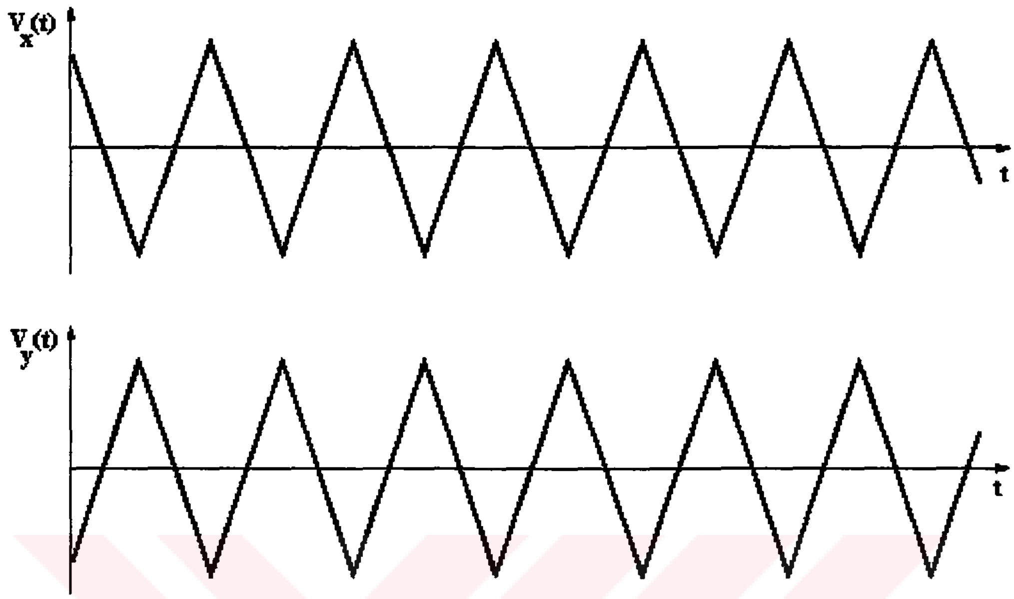

Figure 1.10 The reference voltages used in the comparators. (Chapman,2002)

If a sinusoidal control voltage is applied to the circuit as shown in Figure 1.11, the width of resulting pulse train varies sinusoidally with the control voltage. The result is a high-power output waveform whose average voltage over any small region is directly proportional to the average voltage of the control signal in that region. The fundamental frequency of the output waveform is the same as the frequency of the input control voltage. Figure 1.12 shows PWM inverter voltage and current waveform.

A complete three-phase PWM inverter would consist of three of a single-phase inverter which is described above with control voltages consisting of sinusoids shifted by 120^0 between phases. Frequency control in a PWM inverter of this sort is accomplished by changing the frequency of the input control voltage.

A PWM inverter switches states many times during a single cycle of the resulting output voltage. Reference voltages with frequencies as high as 12 kHz are used in PWM inverter designs, so the components in a PWM inverter must change states up to 24.000 times per second. This rapid switching means that PWM inverters require faster component such as GTO thyristors, IGBTs or power transistors for proper operation.

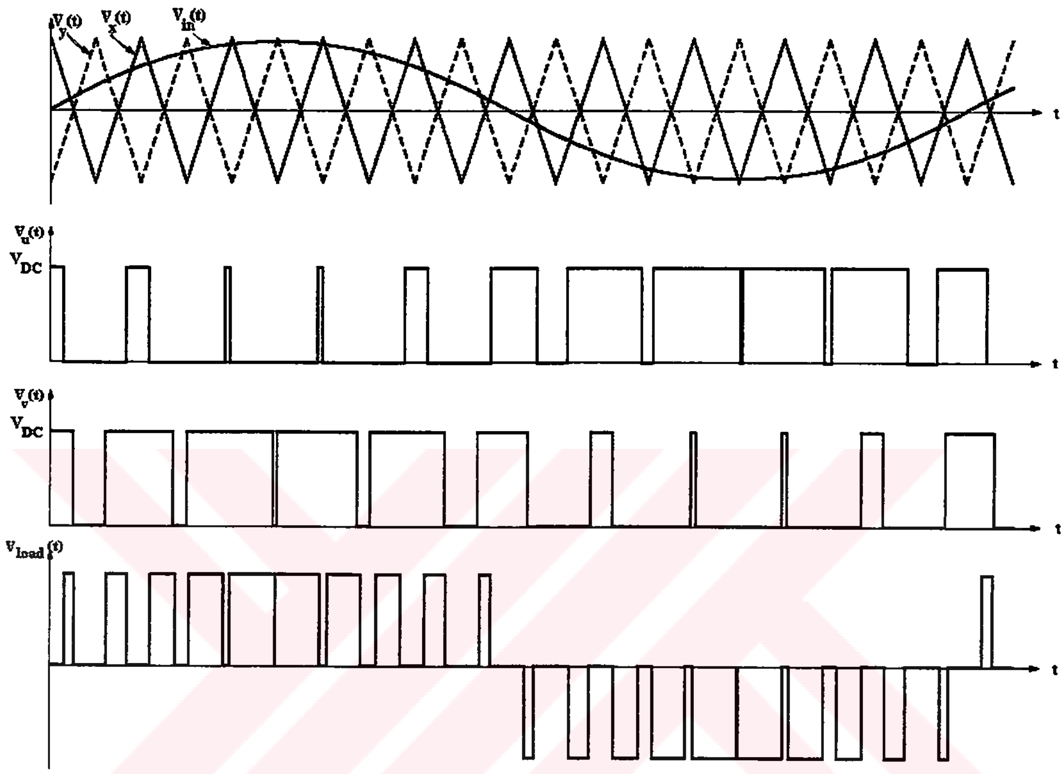

Figure 1.11 The output of the PWM circuit with a sinusoidal control voltage applied to its input. (Chapman,2002)

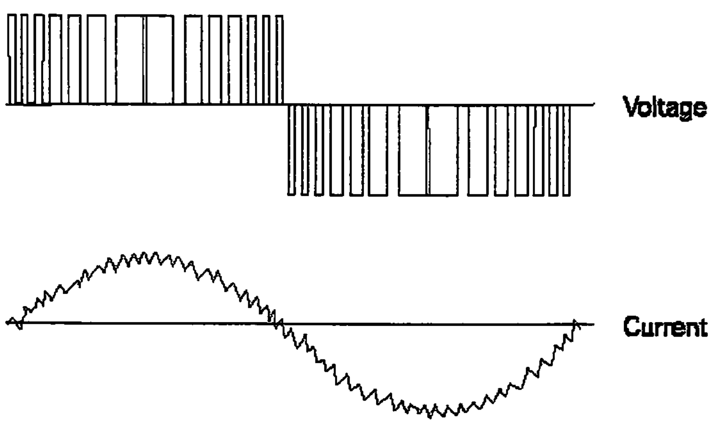

Figure 1.12 PWM inverter output voltage and current waveform. (Siemens)

The switching devices are turned on for longer periods of time. Voltage and current which is shown in Figure 1.11 build up in the motor increases.

Advantages of PWM inverter include good power factor through a speed range from 0 to 100 percent and low harmonic distortion generation on power systems. It can control several motors from a single drive, can be tested without being connected to a motor and has fast response and close control characteristics. Disadvantages include no regenerative braking capability, need for greater skill in servicing, greater motor heating due to motor harmonic distortion generation and limited cable distance between drive and motor (50-100 feet).

A cycloconverter, whose block diagram is shown in Figure 1.13, is constructed from a number of semiconductor devices connected in such a way so that AC power at one input frequency can be converted to AC power of varying frequencies. This is achieved using phase-control. The phase-controlled cycloconverters are capable of providing a variable voltage/variable frequency power supply for driving AC machines, due to their ability to operate in all 4 quadrants of the V-I plane.

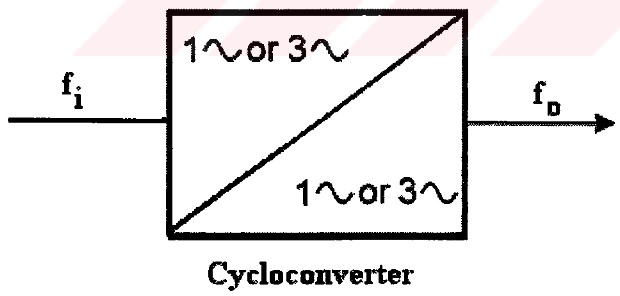

Figure 1.13 Block Diagram of a cycloconverter (Ozpineci and Tolbert)

To understand the operation principles of cycloconverters, the single-phase to single-phase cycloconverter which is shown in Figure1.14 should be studied first. This converter consists of back-to-back connection of two full-wave rectifier circuits. Figure 1.15 shows the operating waveforms for this converter with a resistive load.

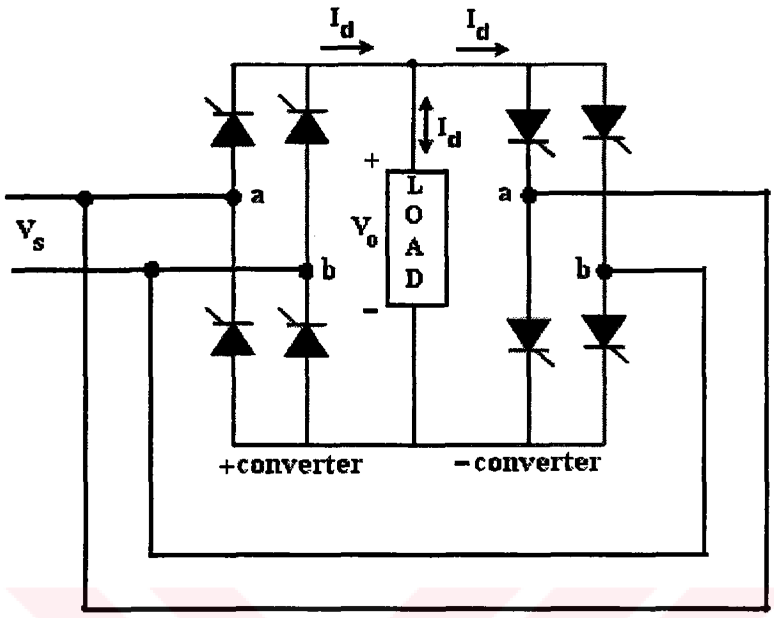

Figure 1.14 Single-phase to single-phase cycloconverter (Ozpineci and Tolbert)

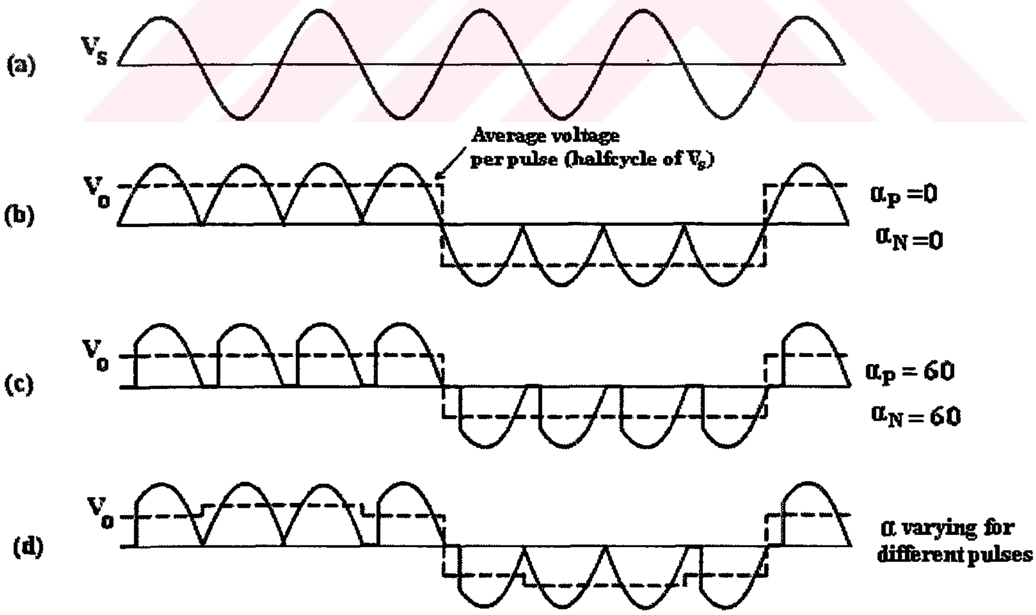

Figure 1.15 Single-phase to single-phase cycloconverter waveform. (Ozpineci and Tolbert)

The input voltage, Vs is an ac voltage at a frequency, f_i as shown in Figure1.15a. For easy understanding assume that all the thyristors are fired at α=0° firing angle, i.e. thyristors act like diodes. Note that the firing angles are named as α_P for the positive converter and α_N for the negative converter. Consider the operation of the cycloconverter to get one-fourth of the input frequency at the output. For the first two cycles of V_s, the positive converter operates supplying current to the load. It rectifies the input voltage. Therefore, the load sees 4 positive half cycles as seen in Figure 1.15b. In the next two cycles, the negative converter operates supplying current to the load in the reverse direction. The current waveforms are not shown in the figures because the resistive load current will have the same waveform as the voltage but only scaled by the resistance. Note that when one of the converters operates the other one is disabled, so that there is no current circulating between the two rectifiers.

The frequency of the output voltage, V_0 in Figure 1.15b is 4 times less than that of V_s i.e. f_o / f_i = 1/4. Thus, this is a step-down cycloconverter. Similarly, cycloconverters that have f_o / f_i >1 frequency relation are called step-up cycloconverters. Step-down cycloconverters are more widely used than the step-up ones.

In principle, cycloconverters can have any combination of input and output phase numbers, but in practice the 3-phase input, 3-phase output version which is shown in Figure 1.16 is the most common and a typical output for one phase is shown in Figure 1.17. This output is produced when the cycloconverter is being modulated with a sinusoidal reference so as to fabricate a mean sinusoidal output voltage.

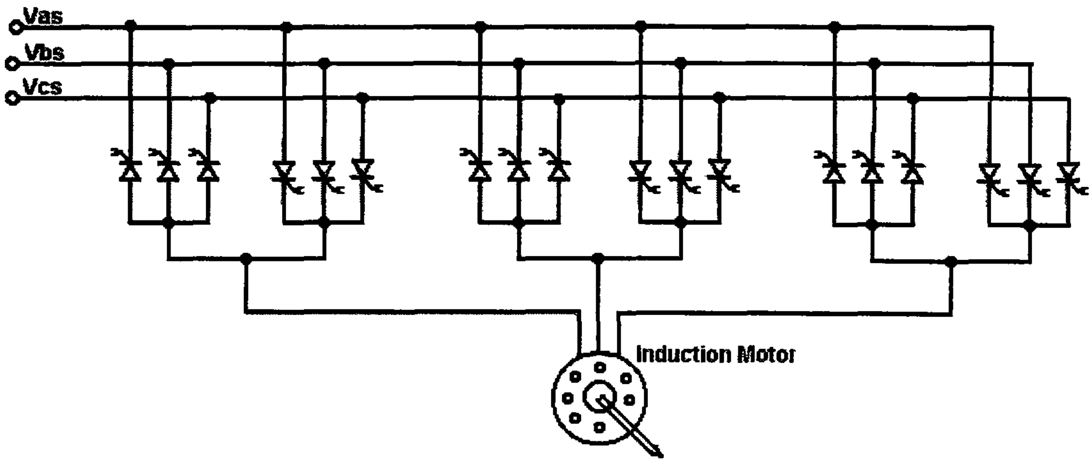

Figure 1.16 Typical 18-Thyristor 3-Phase Input, 3-Phase Output Cycloconverter (http://murray.newcastle.edu.au)

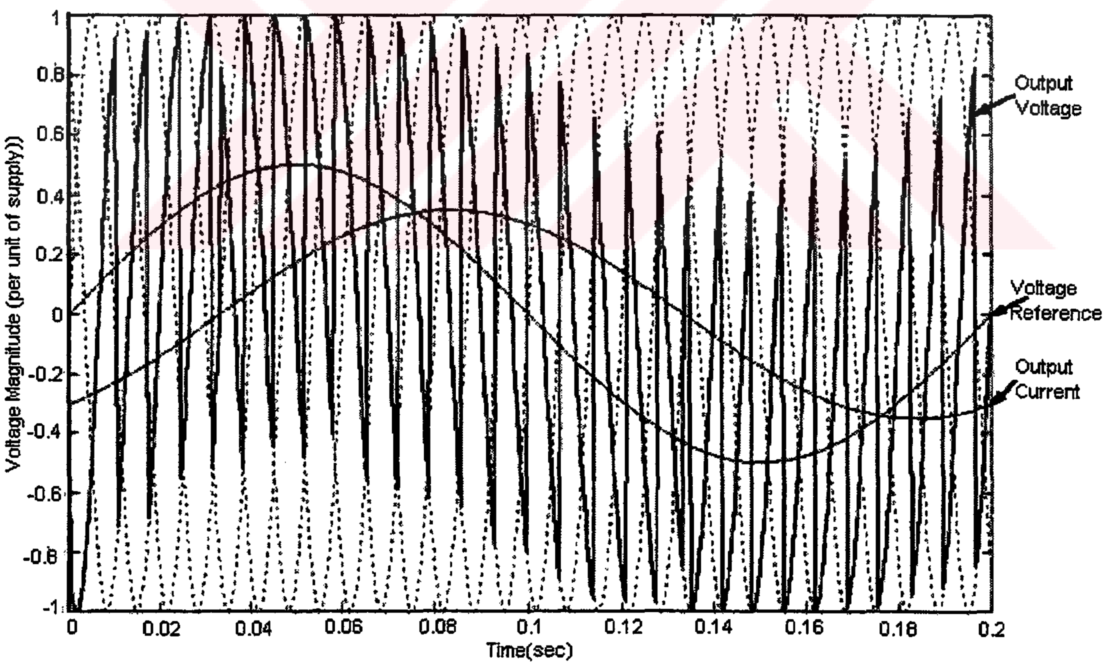

Figure 1.17 Output Voltage and Mean Current Waveforms of an 18-Thyristor Cycloconverter (http://murray.newcastle.edu.au)

1.4. Investigation Undertaken

The main objective of the work described in this thesis is to investigate the performance of an induction motor over its useful speed range, and also its performance at the lower and higher ends of that range. The current accepted range for a 50 Hz, motor is from 10 to 100 Hz, with deteriorated performance at the ends of this range. The particular voltage/frequency source is by PWM control.

After induction motor parameters are obtained, equivalent circuit of motor is constructed and a computer is coded to simulate the motor performance witth pure AC on different loads over a frequency range of 10 Hz-100 Hz. Then PWM source supplied to the motor on same frequencies and results are monitored and compared with pure AC.

2. ANALYTICAL INVESTIGATION

Although induction motors are mainly used in open-loop, constant speed applications, they are also used in adjustable ac drive systems, because of their robust and simple construction. So, it is important to understand their characteristics such as current, torque, power, losses and so on.

2.1. Equivalent Circuit of a 3-Phase Induction Motor

It is possible to construct the equivalent circuit of an induction motor. The equivalent circuit shown in Figure 2.1 (Bose(a),1986) is very important for steady-state performance analysis.

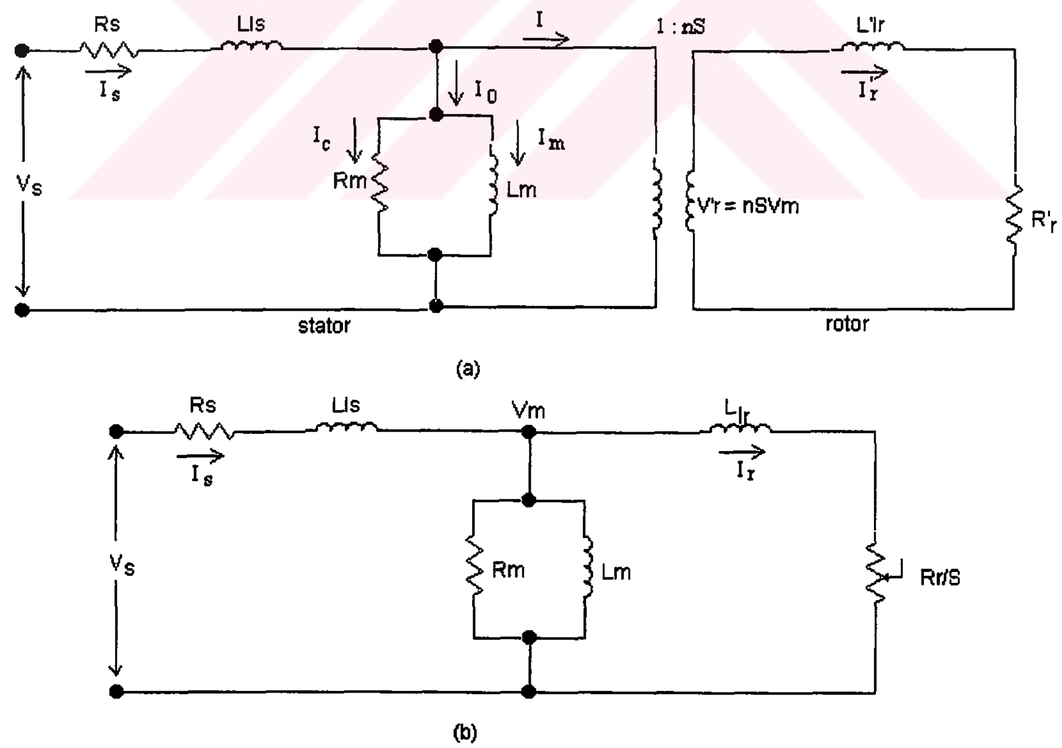

Figure 2.1 The Per-phase equivalent circuit of an induction motor

The fundamental components of induction motor are the stator and rotor.

When balanced three phase voltages are applied to the windings of the stator, balanced currents flow in the three interconnected phase windings. These currents produce a magnetic field in stator and current is induced in the rotor by induction or transformer action. The induction of voltage and currents in the rotor circuit of an induction motor is essentially a transformer operation. So, the equivalent circuit of an induction motor is similar to the equivalent circuit of a transformer.

In figure 2.1(a) a counter emf V_m, is generated by the synchronously rotating air gap flux wave. Then this emf converted to slip voltage $V_r' = nSV_m$ in the rotor phase winding. Here, n is the rotor to stator turns ratio and S = slip. Due to voltage drop in resistance R_s and leakage inductance L_{ls}, the stator terminal voltage V_s differs from voltage V_m. The no-load excitation current I_0 consist of two components. One of them is a core loss component $I_c = V_m/R_m$ and the other is magnetizing component $I_m = V_m/w_eL_m$, R_m is the equivalent resistance for excitation loss and L_m the magnetizing inductance. The rotor induce voltage V'_r causes rotor current I'_r at rotor slip frequency w_{sl}, which is limited by rotor resistance R'_r and leakage impedance $w_{sl}L'_{lr}$. The stator current I_s has two components which are the excitation component I_0 and the rotor reflected current I_r. The equivalent circuit with respect to the stator is shown in Figure 2.1 (b) , where I_r is given as

$$I_r = nI'_r = \frac{n^2SV_m}{R'_r + jw_eL'_{lr}} = \frac{V_m}{\left(\frac{R_r}{S}\right) + jw_eL_{lr}} \qquad (2.1)$$

where the parameters R_r and L_{lr} are referred to the stator. The difference in rotor mechanical speed versus magnetic field rotational speed is known as "slip." The variable resistor "R_2/S" represents the way slip causes increased current. The greater the slip, the lower the value of this resistance, and the more current flows in this branch of the circuit and therefore at standstill, S = 1. Figure 2.1 (b) corresponds to the short-circuited transformer equivalent circuit. When the slip is almost zero at a "no-load" condition (near synchronous speed i.e., S ~ 0), "R_2/S" is seen to be a very high value. As a result, the current can be thought of as all going through the "L_m" or magnetizing branch of the circuit. The current $I_r = 0$ and the machine takes the excitation current I_0 only. At a subsynchronous speed(0<S<1) and with a small value of S, the rotor current I_r is principally influenced by R_r/S ($R_r/S >> w_e L_{lr}$).

2.2. Torque/Speed and Current/Speed Equations

The equivalent circuit of an induction motor can be used to obtain a general expression for torque and current as a function of speed. For this, the loss and power expressions of a machine can be written:

input power	$P_{in} = 3V_s I_s \, Cos\Phi$	(2.2)
stator copper loss	$P_{ls} = 3\, I_s^2 \, R_s^2$	(2.3)
core loss	Plc = 3(Vm2/Rm)	(2.4)
power across air gap	Pg = 3 Ir2 (Rr/S)	(2.5)
rotor copper loss	$P_{lr} = 3\, I_r^2 \, R_r$	(2.6)
output power	$P_0 = P_g - P_{lr} = 3\, I_r^2 \, R_r\, (1\text{-}S)/S$	(2.7)
shaft power	$P_{sh} = P_0 - P_{fw}$	(2.8)

The output power is product of developed torque T_e and speed, So, T_e can be expressed as

$$T_e = \frac{P_0}{w_m} = \frac{3}{w_m} I_r^2 R_r \frac{1-S}{S} = 3\left(\frac{P}{2}\right) I_r^2 \frac{R_r}{S w_e} \tag{2.9}$$

where $w_m = (2/P)w_r$ is the rotor mechanical speed (rad/s). Substituting equation (2.5) in (2.9) yields

$$T_e = \left(\frac{P}{2}\right)\frac{P_g}{w_e} \tag{2.10}$$

equation (2.10) indicates that torque can be calculated from the air gap power by knowing the stator frequency. The power P_g is often defined as torque in synchronous watts.

The equivalent circuit of Figure 2.1(b)(Bose(a),1986) can be simplified to Figure 2.2(Bose(a),1986) where the core-loss resistor R_m has been neglected and magnetizing inductance L_m has been transferred to the input. The approximation is valid for an integral-horsepower machine where $|(R_s + jw_e L_{ls})| << w_e L_m$ .In figure 2.2 current I_r can be solved as

$$I_r = \frac{V_s}{\sqrt{(R_s + R_r / S)^2 + w_e^2 (L_{ls} + L_{lr})^2}} \tag{2.11}$$

and substituting equation (2.11) in (2.9) yields

$$T_e = 3\left(\frac{P}{2}\right)\frac{R_r}{w_e}\frac{V_s^2}{(Rs + Rr / S)^2 + w_e(Ll_s + L_{lr})} \tag{2.12}$$

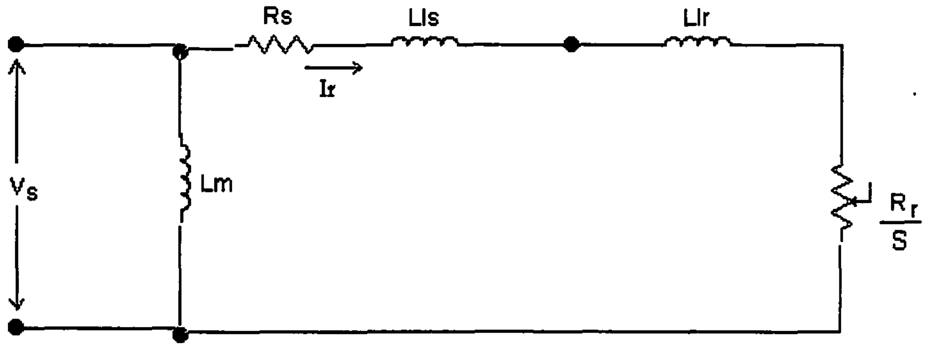

Figure 2.2 Approximate equivalent circuit

If the voltage and frequency are constant, the torque then can be calculated as a function of slip s from equation (2.12), and the torque-speed(w_r / w_s =1-s) curve, where the value of slip is extended beyond the region $0 \leq s \leq 1$ can be drawn. This is shown in figure 2.3(Bose(a),1986). In this figure, motor operates three regions. These are defined as plugging ($1 \leq s \leq 2$) motoring ($0 \leq s \leq 1$) and regeneration($s < 0$).

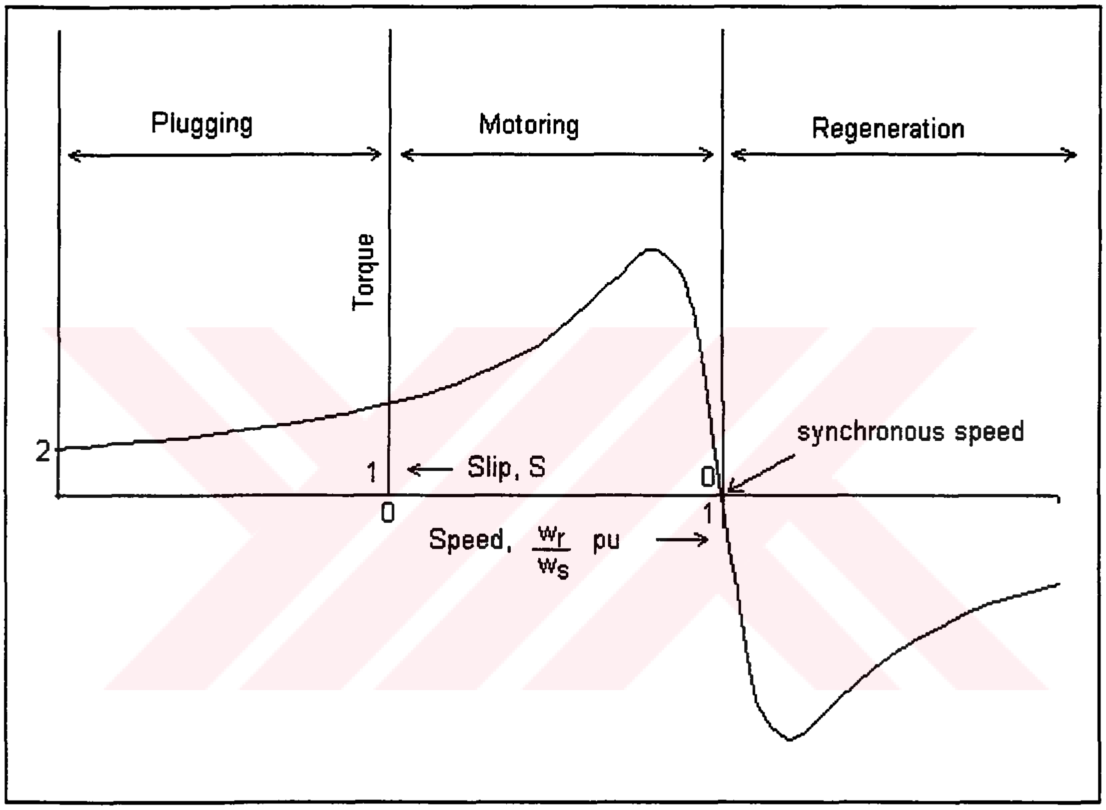

Figure 2.3 Torque-speed curve at constant voltage and frequency.

Although there are several ways to use the equivalent circuit of an induction motor for current I_r and torque T_e, the easiest method is first to determine the Thevenin equivalent of the circuit. Thevenin's theorem states that any linear circuit that can be separated by two terminals from the rest of the system can be replaced by a single voltage source in series with an equivalent impedance. If it is done to the equivalent circuit of induction motor and the core-loss resistor R_m has been neglected, the resulting Thevenin equivalent circuit would be as shown in figure 2.4(c)(Chapman,2002).

Figure 2.4(a) (Chapman,2002) shows the open terminals used to find the V_{th} which is called as Thevenin voltage.

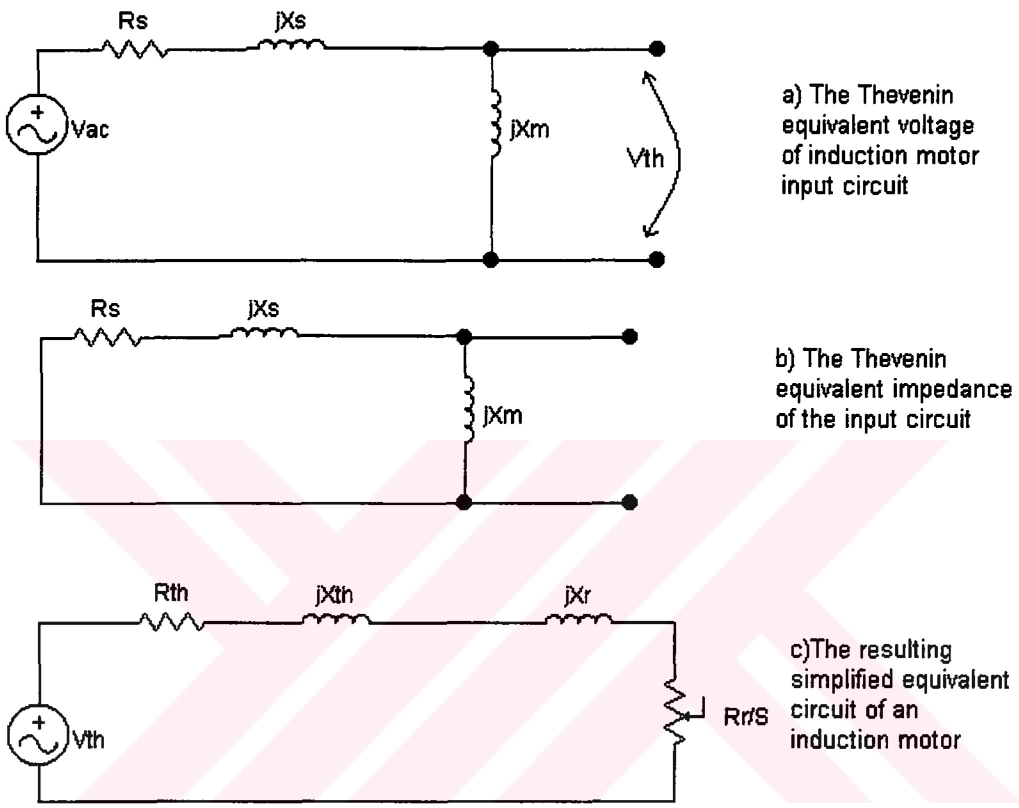

Figure 2.4 Thevenin equivalent circuit

$$V_{th} = V_{ac} \frac{Z_m}{Z_m + Z_s} = V_{ac} \frac{jX_m}{jX_m + R_s + jX_m} = V_{ac} \frac{X_m}{\sqrt{R_s^2 + (X_s + X_m)^2}} \tag{2.13}$$

and V_{th} can be expressed with good accuracy as

$$V_{th} = V_{ac} \frac{X_m}{X_m + X_s} \tag{2.14}$$

because of the magnetization reactance $X_M >> X_s$ and $X_M >> R_s$. Figure 2.4(b) shows the Thevenin impedance which is expressed,

$$Z_{th} = \frac{Z_s Z_m}{Z_s + Z_m} = \frac{jX_m(R_s + jX_s)}{R_s + j(X_m + X_s)} = R_{th} + jX_{th} \tag{2.15}$$

and since $X_m >> X_s$ and $X_m + X_s >> R_{s}$, teh. the Thevenin resistance can be expressed as,

$$X_{th} = X_s \quad and \quad R_{th} = R_s\left(\frac{X_m}{X_m + X_s}\right)^2 \tag{2.16}$$

resulting equivalent circuit is shown in Figure 2.4(c) (Chapman,2002) and from this circuit I_r is expressed below as,

$$I_r = \frac{V_{th}}{Z_{th} + Z_s} = \frac{V_{th}}{R_{th} + (R_2/s) + j(X_{th} + X_s)} \tag{2.17}$$

and magnitude of I_r ,

$$I_r = \frac{V_{th}}{\sqrt{(R_{th} + R_2/s)^2 + (X_{th} + X_s)^2}} \tag{2.18}$$

finally the rotor-induced torque T_{eth} in Thevenin equivalent circuit is expressed as,

$$T_{eth} = \frac{3V_{th}^2 R_2/s}{w_s\left((R_{th} + R_2/s)^2 + (X_{th} + X_s)^2\right)} \tag{2.19}$$

2.3. Variable Voltage/Variable Frequency Equations

A simple and economical method of speed control of induction motors is to vary the stator voltage at constant frequency which is sometimes done with small motors such as driving fans. The motors with a fairly high slip are normally used in this speed control method. The developed torque per ampere of stator current is reduced as the stator current is reduced and for a constant-load torque stator current increases as the speed reduces and this increase in current causes more rotor copper loss and machine heating problems. Figure 2.5(Bose(a), 1986) shows torque-speed curves which have been drawn from equation (2.12) with variable stator voltage and a load torque curve for a fan or blower type drive. In this figure, the intersections define stable points of variable-speed operation.

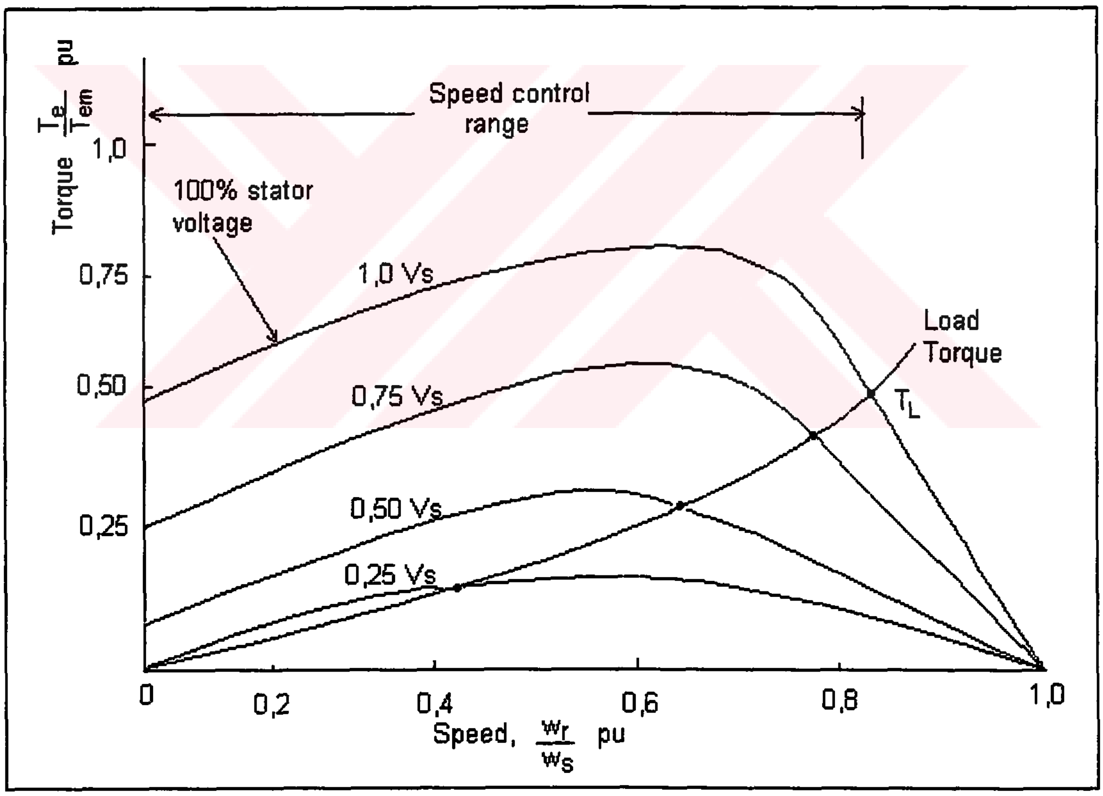

Figure 2.5 Torque-speed curves with variable stator voltage (Bose(a),1986)

If the frequency applied to the stator of an induction motor is changed, the synchronous speed of the motor changes in direct proportion to the change in frequency and torque-speed characteristic curve changes with it as shown in Figure

2.6(Bose(a), 1986) which is plotted from equation (2.12). It is possible to control the speed of the motor either above or below synchronous speed. Nevertheless, It is important to maintain certain voltage and torque limits on the motor as the frequency is varied. For safe operation, when running at speeds below the base speed of the motor, it is necessary to change the terminal voltage applied to the stator for proper operation. If not, the steel in the core of motor saturates and excessive magnetization currents flows in the machine. Therefore the region below the base frequency w_b should be accompanied by the corresponding reduction of stator voltage so as to maintain constant air gap flux. In a variable-voltage, variable-frequency drive system, the machine usually has a low slip characteristic, giving improved efficiency. In spite of the low inherent starting torque for base-frequency operation, an induction motor can always be started at maximum torque as shown in figure 2.7(Bose(a), 1986)

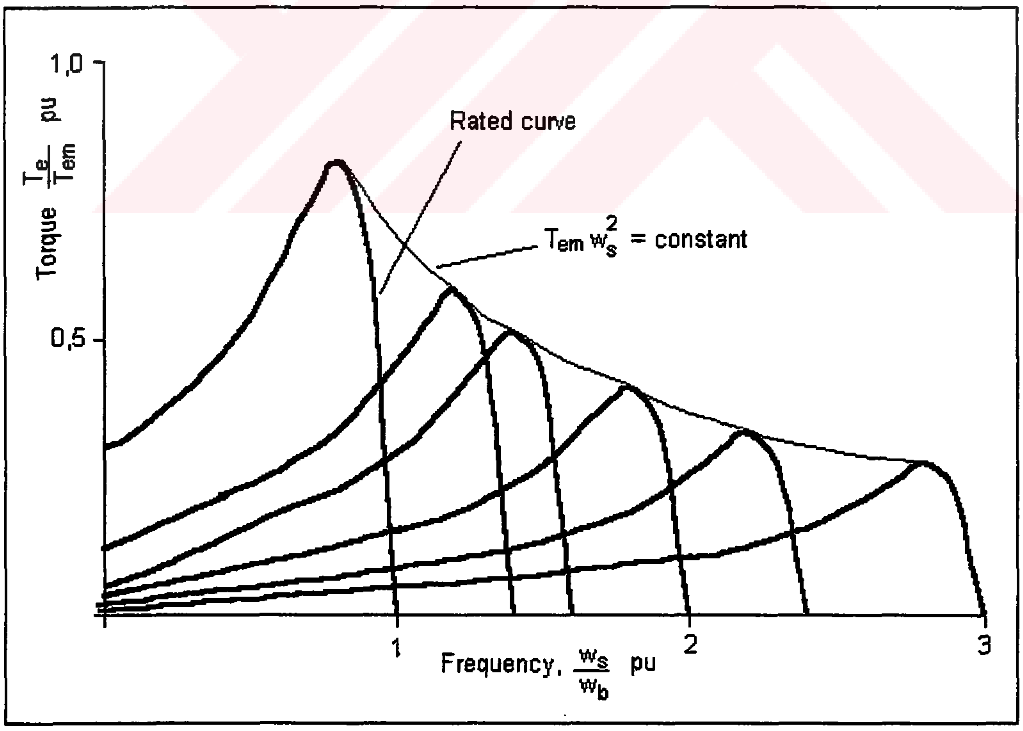

Figure 2.6 Torque-speed curves at variable frequency.

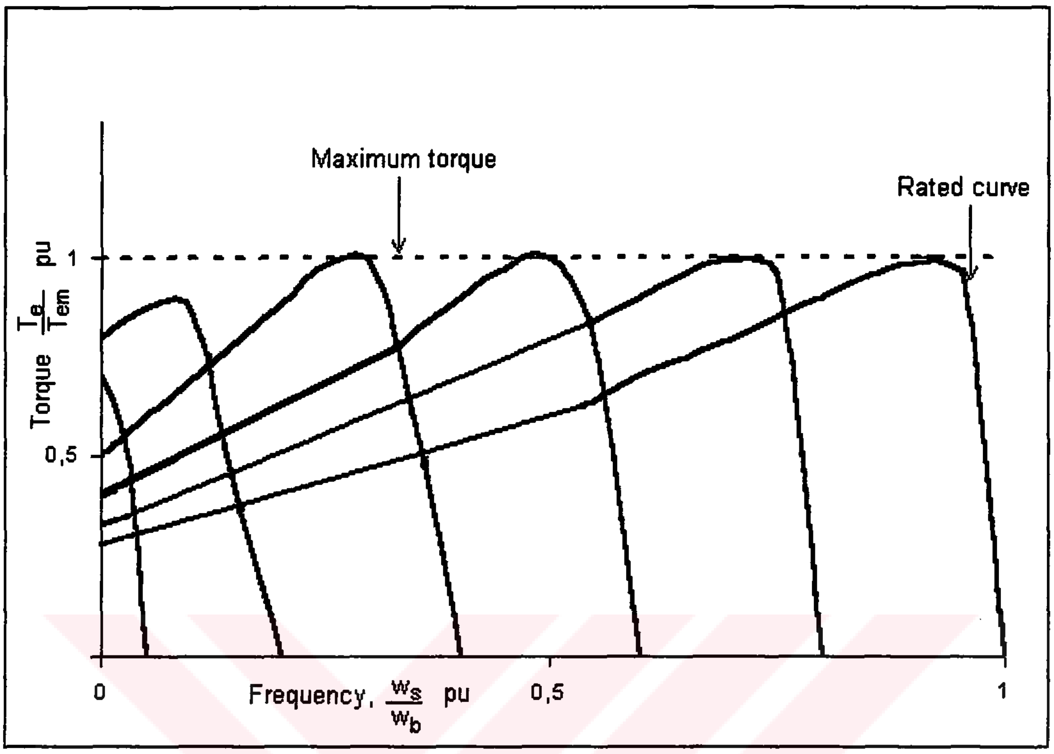

Figure 2.7 Torque-speed curves at constant volt/hertz (Bose(a),1986)

When the frequency is increased above the base speed of the motor, the stator voltage is often held constant at the rated value. Although saturation considerations would permit the voltage to be raised above the rated value under these circumstances, it is limited to the rated voltage to protect the winding insulation of the motor. Figure 2.8 (Bose(a), 1986) shows the different regions of torque-speed curves of a practical drive system with a variable-voltage, variable-frequency supply.

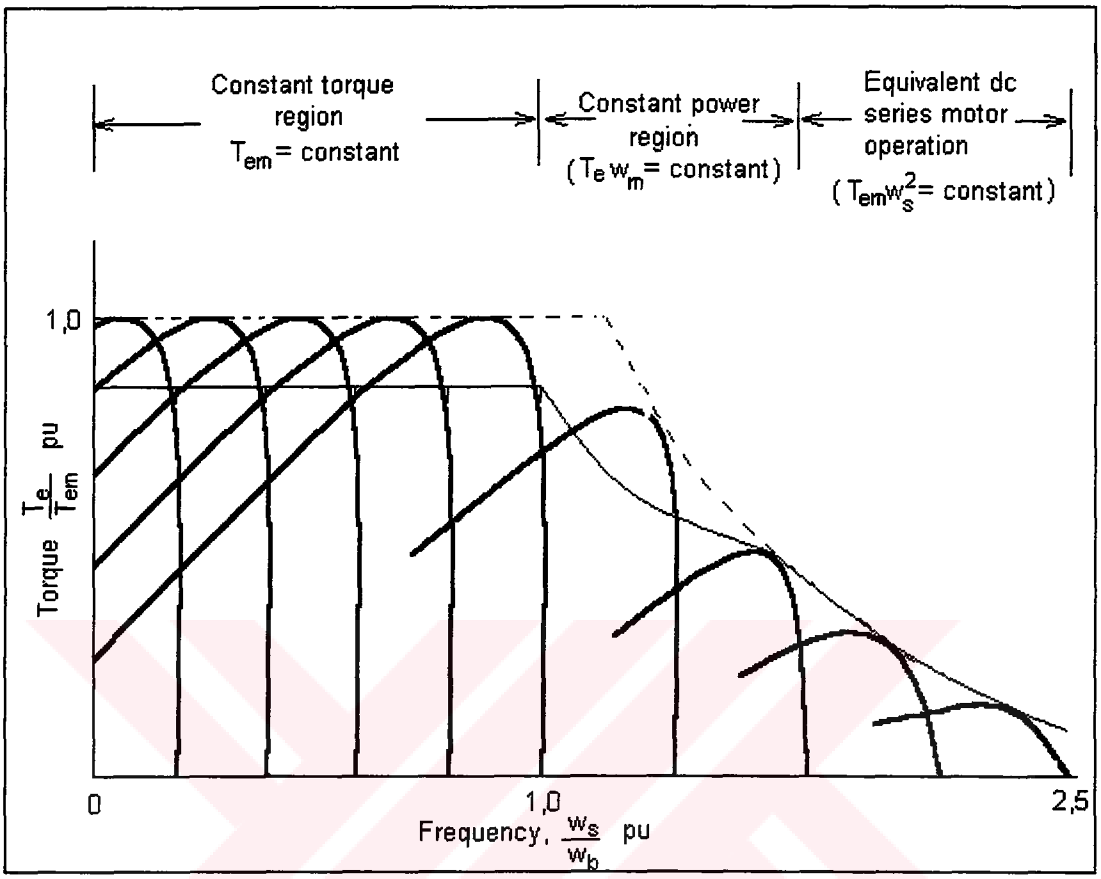

Figure 2.8 Region of torque-speed curves with variable-voltage, variable-frequency power supply (Bose(a),1986)

3. EXPERIMENTAL INVESTIGATION

In order to investigate the performance of an induction motor, whose description and rating are given below in 3.1, first the requirement some was to obtain motor parameters for an equivalent circuit. This was then followed by variable frequency tests.

3.1. Motor Description, Rating

The TecQuipment NE7010 Electrical Machines Test Bench which provides comprehensive console facilities with a wide range of instrumentation to enable extensive investigation of DC and AC motors and generators was used for all experimental tests. This test bench contains an induction motor and dc generator. The characteristics of these machines are as follows respectively.

Type:	Squirrel Cage Induction Motor
Frame Num.:	ST90SC4-01323
Power:	1,1 kW
Volts:	230/400 V
Phase:	3
Frequency:	50 Hz
Amps.:	4,8/2,8 A
Cos φ :	0,76
Rpm:	1390(4-Pole)
Ins. Class	F

Type:	DC Generator
Frame Num.:	3372180-9522
Power:	1,5 kW
Armature V:	220 V

Excitation V: 130 V

Amps.: 8,5 A

Ins. Class F

This induction motor which is coupled to DC generator is used for all load experiment.

3.2. Test for Parameters

The induction motor was load tested with mains pure ac supply at 50 Hz to establish performance guidelines. The resulting torque/speed curve at this operating frequncy is given in Figure 3.1 Additionally, the induction motor was tested for parameters to determine equivalent circuit parameters. These are DC tests for stator resistance, No-Load and Locked-Rotor tests. The procedure used is fairly standard and is adopted from (Chapman,2002). All of the calculations and parameters are given in Appendix A.I.

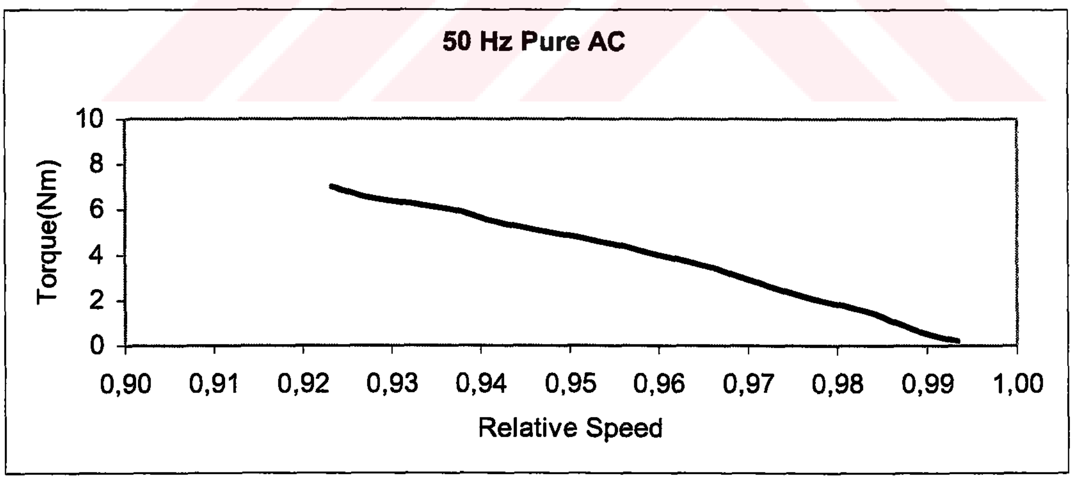

Figure 3.1 Torque/speed characteristic for pure AC test at 50 Hz

3.3. Variable Frequency Tests

Variable frequency test were implemented at 10, 20, 30, 40, 50, 60, 70, 80 and 90 Hz by using a PWM supply. Torque/speed curves and waveforms are monitored. Additionally, harmonics at 50 and 70 Hz were monitored.

3.3.1. PWM Source Description

The TecQuipment MPM1015 Variable frequency Inverter was used for PWM source. This equipment converts an ac power supply, of constant voltage and frequency, into a variable frequency three-phase supply suitable for driving an induction motor at different speeds. Its technical specifications are as follow:

Input Supply:	Single-Phase, 220/240 V ± 6%, 50/60 Hz
Output Supply:	PWM 3Phase, 150W-1.5 kW
Frequency Range:	2-100 Hz, ± 5%
Control Method:	PWM Sinewave, 2-100 Hz

3.3.2. Test Undertaken and Results

To investigate the induction motor performance at variable frequency, it was tested from 10 Hz to 100 Hz by increasing frequency in 10 Hz steps. For this implementation, the induction motor which is coupled to DC generator was supplied by PWM inverter. Block diagram and photo of system is given below and the resulting torque/speed curves are given in Appendix A.II.

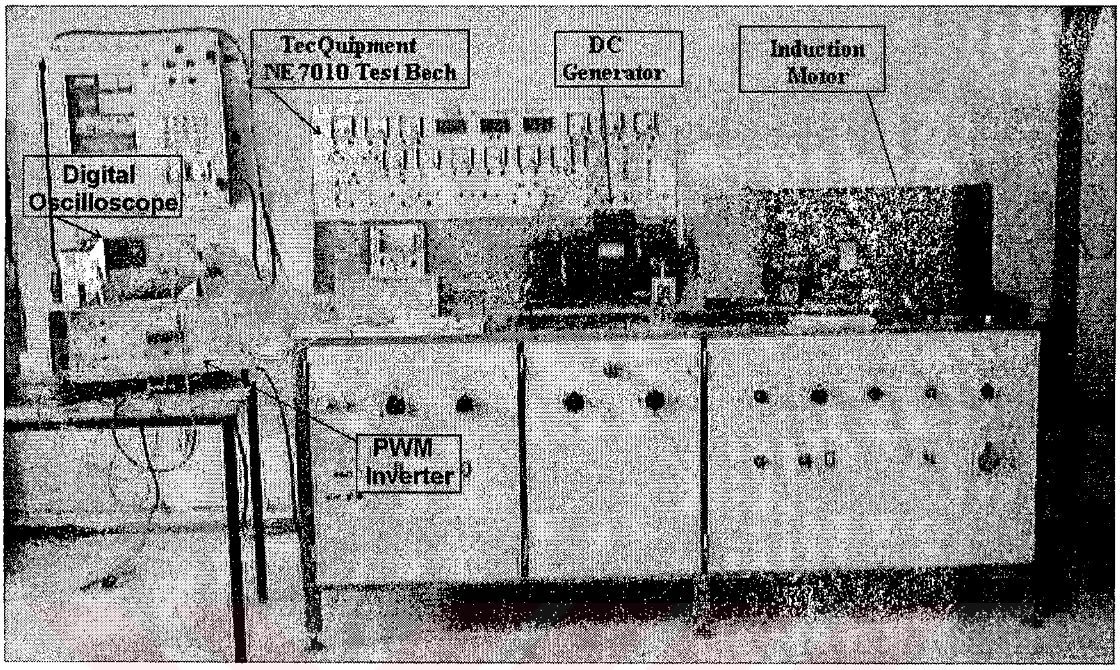

Figure 3.2 Experimental Test rig

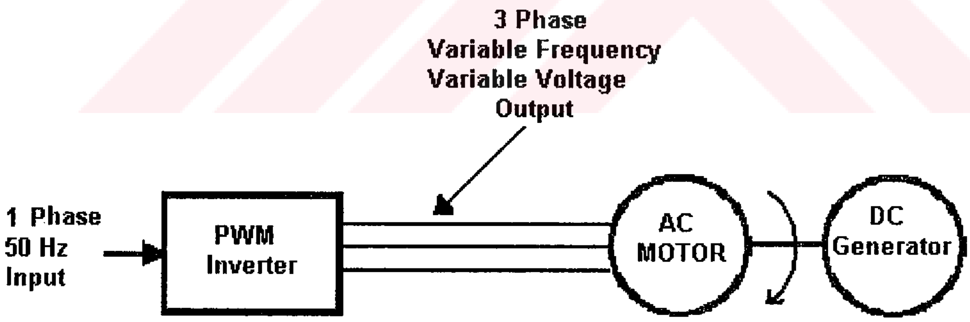

Figure 3.3 Experimental Test Block Diagram

Additionally, at 25 and 50 Hz, the speed was fixed at 750 and 1500 rpm respectively. Then torque was increased by applying load to the induction motor and to maintain speed at same values, the frequency was increased. The resulting responses of PWM inverter are given in figure 3.2 and 3.3 respectively. Its seen from the figures that when torque is increased from 0 to 4.5 Nm, the frequency increases from 50 to 53 Hz. For 25 Hz, when the torque is increased from 0 to 4.3 Nm, the frequency increases from 25 to 27,9 Hz.

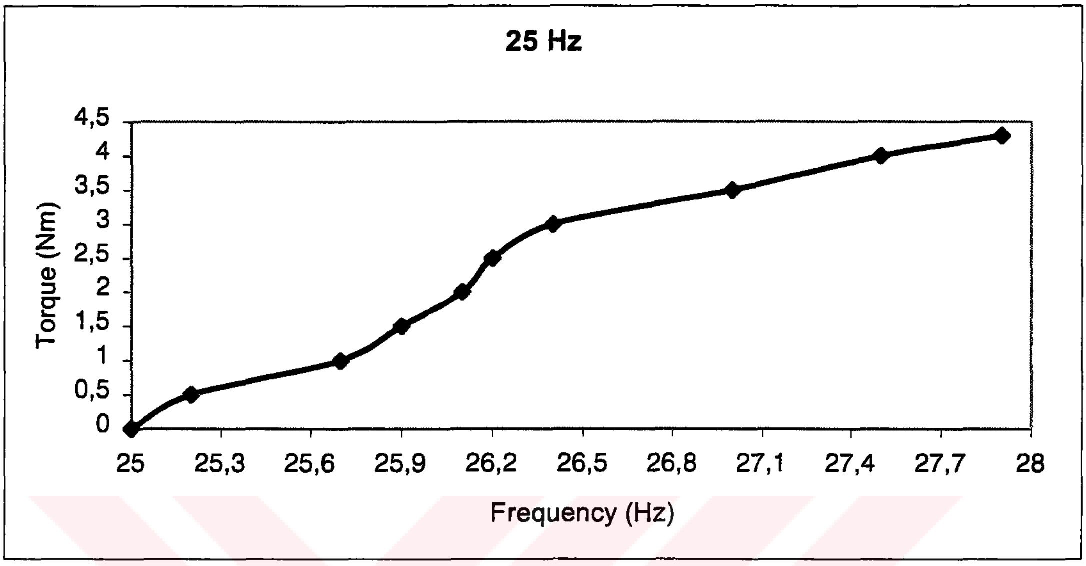

Figure 3.4 Torque/frequency curve at constant 750 rpm. (f=25 Hz)

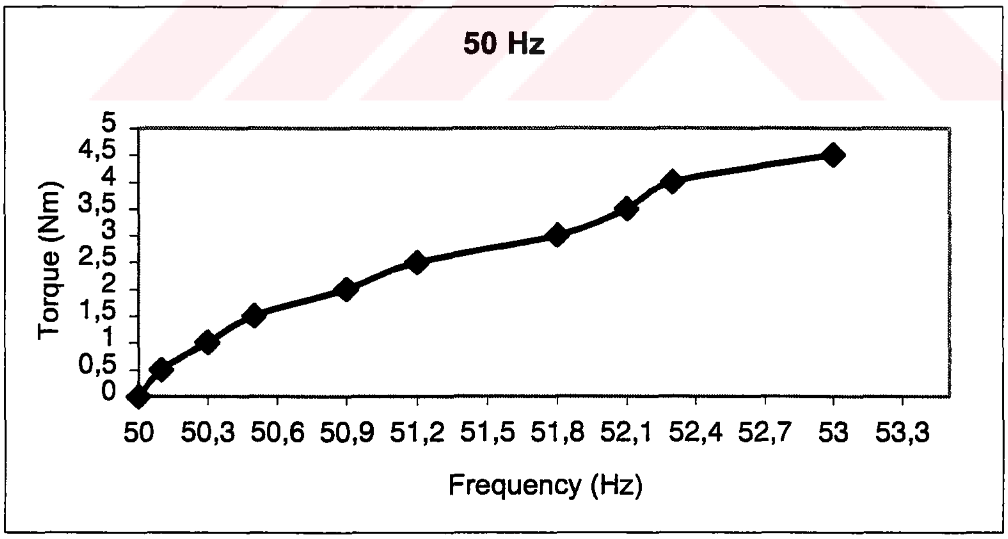

Figure 3.5 Torque/frequency curve at constant 1500 rpm. (f=50 Hz)

3.3.3. Waveforms

To monitor PWM voltage and current waveforms, the output of PWM source was connected a 220:12 Volt step down ac transformer and output of the transformer was connected a digital oscilloscope to monitor voltage waveform. To monitor the current waveform the current output connector of PWM source was used. The obtained current and voltage waveforms are given in Appendix A.III. In each figure, the upper waveform is the voltage and the other is the current. In each case the voltage waveform shows switching with varying pulse widths. This switching, combined with the machine inductive windings, produce the distinctive current wave shape.

The waveforms shown in figure A.III.1 and 2 were monitored at f=20 Hz and at load T=0 Nm and T=3 Nm respectively. It is seen from the figures that the current amplitude can be seen to increase with load. This is due solely to the reduction in speed and not to any change in supply voltage. So the machine automatically regulates the energy it obtains to suit the load conditions. This is also seen from figure A.III.3 and figure A.III.4.

Additionally, it is also seen from figures that the current waveforms show spikes which will be a potential cause of interference to adjacent equipment.

3.3.4. Harmonics

In PWM terminology, the modulation process is recognised as being that process which relates the switching instants of the PWM waveform to the amplitude of the fundamental component. The modulation process which defines this switching strategy may be obtained by Fourier analysis. As suggested by (Besanov,1991), Patel and Hoft have shown that by constraining the PWM waveform to possess odd quarter wave symmetry the amplitude of any harmonic component of the order *n* is given by the following equation (see Appendix VI)

$$V_n = \frac{4}{n\pi}\left\{1 + 2\sum_{i=1}^{k}(-1)^i \cos(n\alpha_i)\right\} \quad for\, 0 < \alpha_i < \frac{\pi}{2} \quad (i = 1,2,3,....,k) \tag{3.1}$$

It is clear from equation 3.1 that the relationship of the switching instant α_i to the amplitude of the fundamental V_1 can be found.

To determine the fundamental voltage and harmonics of PWM waveform, first, output voltage of PWM source was monitored by using an oscilloscope at 50 and 70 Hz. Then switching angles for each frequency tested were determined from the waveform. Finally, fundamental voltage and harmonics were calculated by substituting determined switching angles in equation 3.1. The resulting line frequency spectrums for 50 and 70 Hz are given in figure 3.2 and 3.3 respectively.

3.3.5. Discussion on Limitations and Difficulties

Although computer programs were simulated for a relative speed 1 to 0 for all predicted values of frequency tests, in practice, the load tests for all frequencies were done until current about 4.8 A, which is rated value. If this value were exceeded, the operation will be harmful for motor windings. So, all measurements were done until about 4.5 A for safety operation.

Additionally, usable torque at higher operating frequencies is further reduced since applied voltage was not increased and friction and windage losses are increased. So, measurement range became lower to monitor the response of the machine for reliable comparison with computed results, especially for above 90 Hz. Consequently, load tests were implemented up to 90 Hz and not implemented for 100 Hz.

To analysis and monitor fundamental and harmonic contents of output voltage of PWM source, mathematical (or analytical) method was used, because of the lack of spectrum analyzer. This is done only for 25 and 50 Hz. It was mentioned before at section 3.3.4 about how to implement and calculate this data.

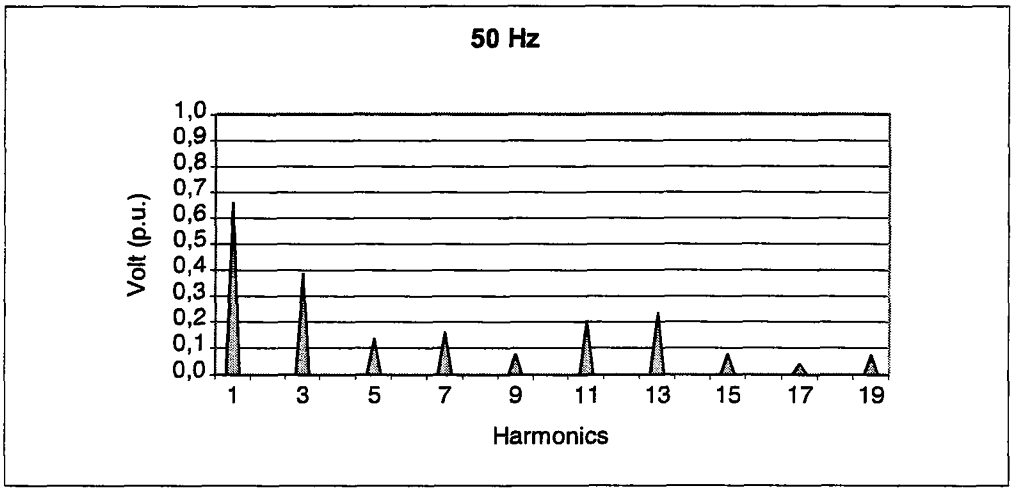

Figure 3.6 Line voltage frequency spectrum at 50 Hz.

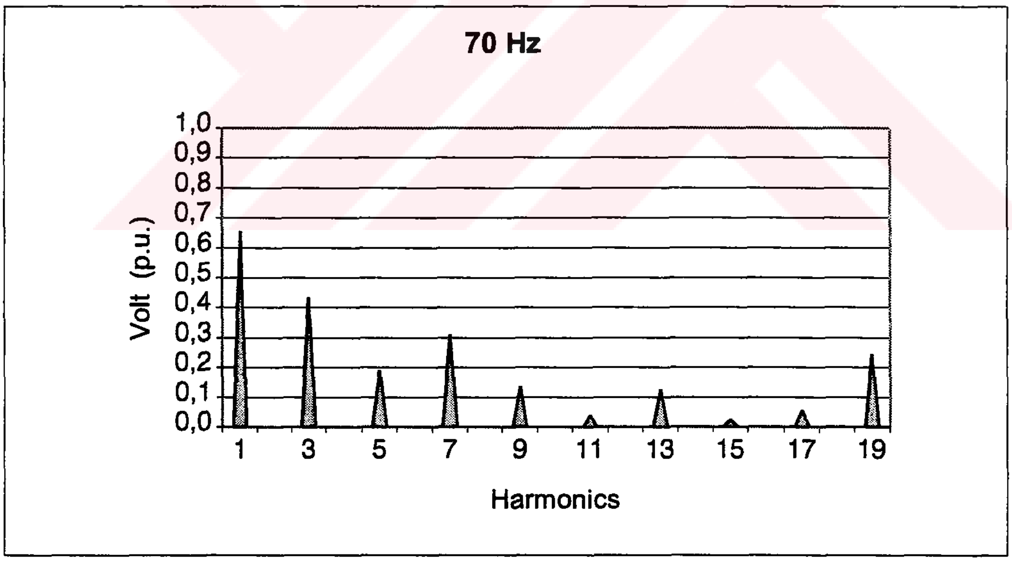

Figure 3.7 Line voltage frequency spectrum at 70 Hz.

4. COMPUTER PROGRAMMES

To simulate performance characteristics of an induction motor, tests for parameters on No-Load and Locked-Rotor were done. The procedure used is fairly standard and is adopted from (Chapman,2002). Two Turbo C++ computer programs which are given in Appendix A.IV, coded on the PC to predict machine performance based on the Thevenin equivalent circuit(Chapman,2002)

4.1. Developed Programme

Two computer programs were coded using Turbo C++ on the PC. One of them is Consvf.cpp which was coded to simulate induction motor performance at constant V/f with pure AC between 0 and 50 Hz and also to compare motor performance with PWM experimental results in the same range. In this program, first, equivalent circuit parameters were accepted at constant values, then Thevenin equivalent was constructed and results such as slip, torque at shaft, output power including losses, power factor, rotor current and Thevenin voltage were written to a txt file.

The other computer program which is Vsabit.cpp and is the same as Consvf.cpp, except that the operation range is from 50 to 100 Hz and voltage is constant at the rated value.

4.2. Results and Evaluation

Simulation results were used as guidelines to establish the accuracy of the results obtained for load testing of the machine The result of these simulations are given in terms of predicted torque/slip. The machine rated torque as calculated from the nameplate is given at 6.25Nm, and rated torque with curves at 10, 20, 30, 40 and 50 Hz at the constant torque region is given in Figure 4.1.

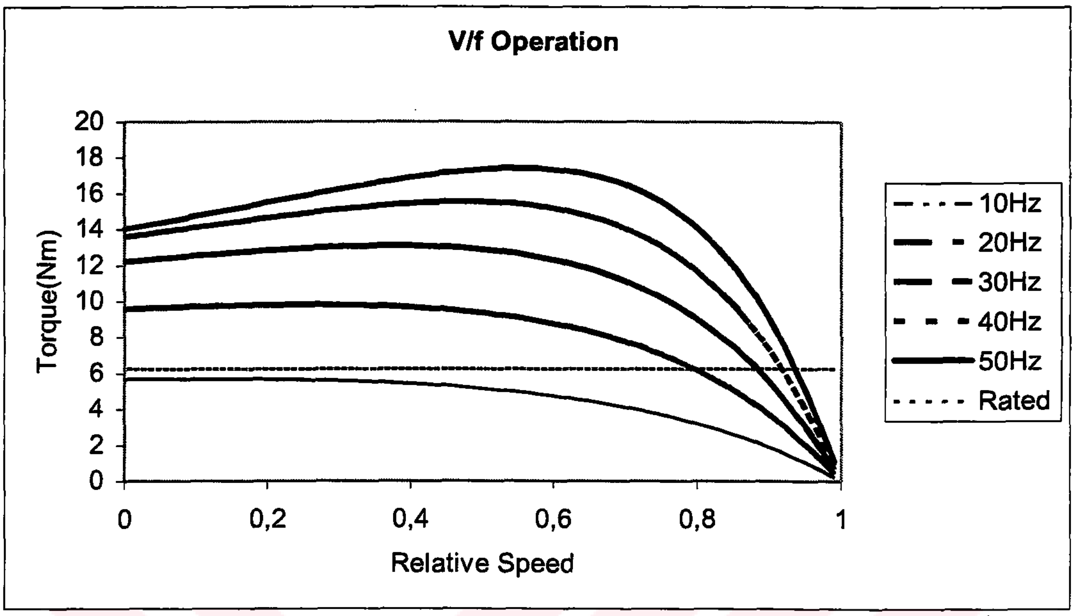

Figure 4.1 Simulation result for variable frequency operation

It is seen from this Figure that maximum available torque is 5,67 and occurs at the relative slip of 0,01 for 10 Hz. This is somewhat lower than the rated value.

At the same time, it is seen from Figure 4.1 that maximum torque for 20, 30, 40 and 50 Hz is 5.67 , 9.8 , 13.07 , 15.53 and 17.38 respectively and these values occur at relative slip .0.01., 0.25 , 0.38 , 0.48 and 0.55 respectively.

The rated torque with curves at 50, 60, 70, 80, 90 and 100 Hz is given in Figure 4.2. It is seen from Figure 4.2 that maximum available torque is 13.42 Nm and occurs at the relative slip of 0,62 for 60 Hz. At the same time, maximum torque for 70, 80, 90 and 100 Hz is 10.44 , 8.35 , 6.83 and 5.69 respectively and this values occur at relative slip .0.66., 0.7 , 0.73 and 0.75 respectively.

Additionally, the induction motor was simulated with pure AC with 50 Hz at 200 Volts by using computer program Vsabit.cpp. Because, PWM actual output voltage was measured as 200 Volts. Resulting torque/speed curve with 50 Hz pure AC at 220 Volts and rated torque are given in figure 4.3 It is seen from Figure 4.3 that maximum available torque is 14.37 and occurs at the relative slip of 0,55 for pure AC 200 Volts.

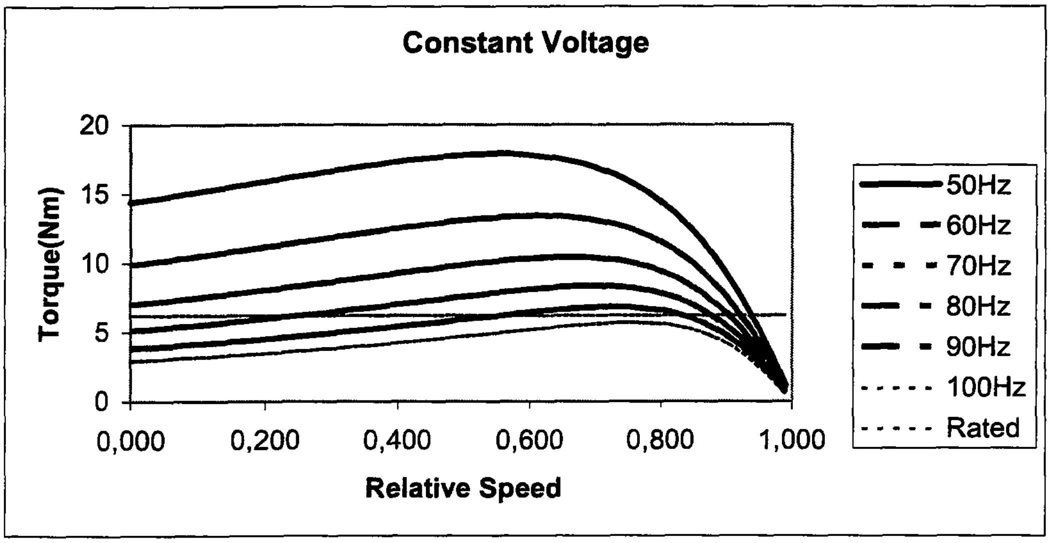

Figure 4.2 Simulation result for constant voltage operation

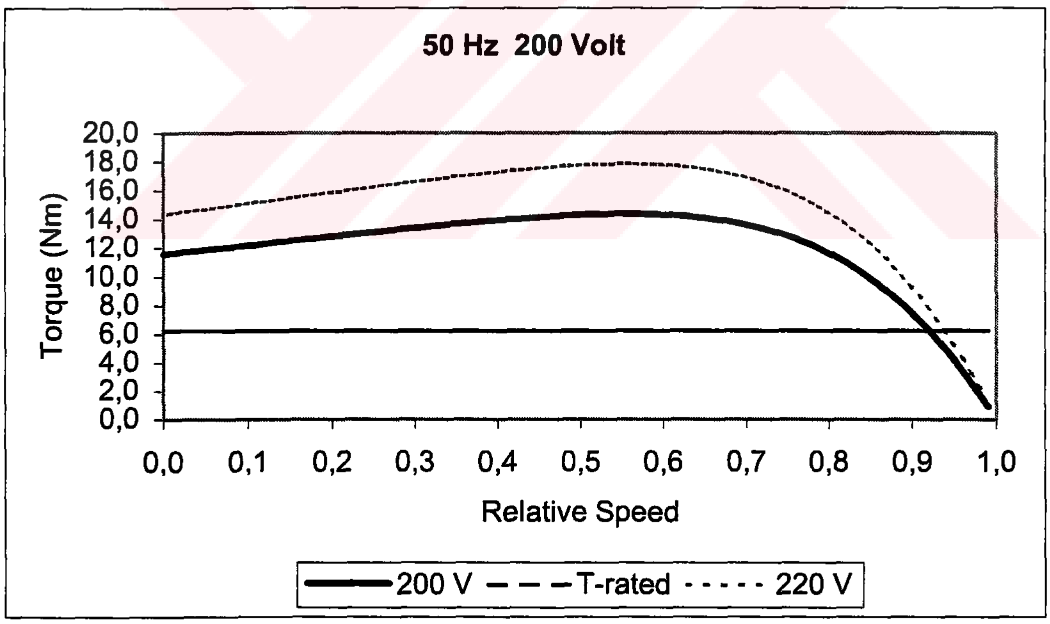

Figure 4.3 Simulation result for pure AC, 50 Hz and 200 Volts with rated torque

5. COMPARISON OF COMPUTED AND PRACTICAL RESULTS

For comparisons, first, the induction motor was load tested with mains pure ac supply at 50 Hz and it was simulated at the same frequency. Then, the induction motor was simulated from 10 Hz to 100 Hz by increasing frequency in 10 Hz steps. This was then followed by variable frequency tests in the same frequencies.

5.1. Accuracy and Comparison with Pure AC Operation

Figure 5.1 shows the predicted and the measured torque/speed characteristic at 50 Hz for the induction motor.

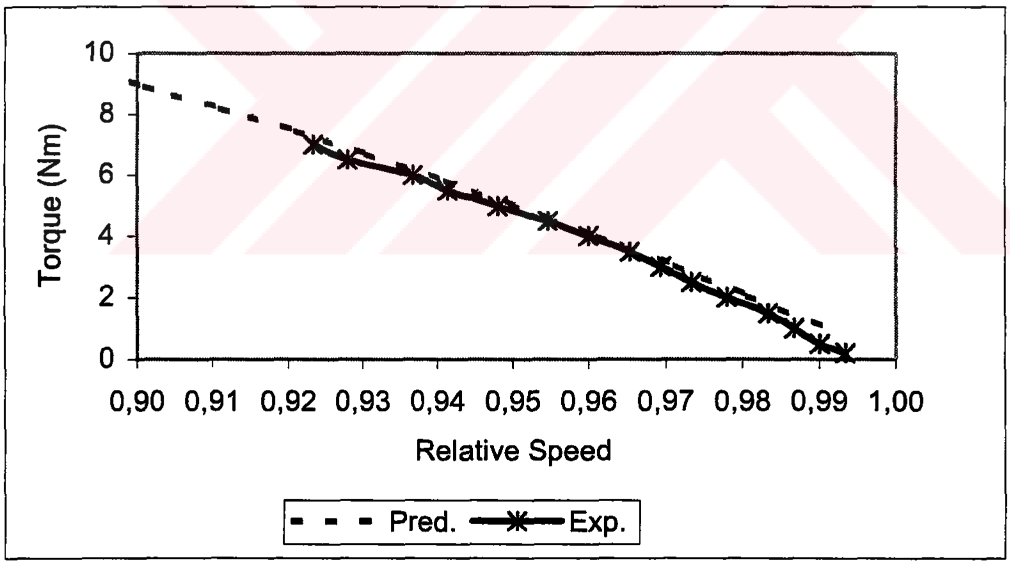

Figure 5.1 Comparison of experimental and predicted torque/speed characteristic of the induction motor f=50 Hz.

It is seen from figure 5.1 that the predicted torque/speed characteristic displays a little higher than that obtained from pure AC testing. This serves to indicate the accuracy in measuring torque which was given above at ± 3 %. This level of accuracy is maintained through the load testing range and consequently the relative machine performance between pure AC and PWM supply should not be affected.

5.2. Comparison of Computed Results with PWM Operation

In the Appendix V, figures A.V.1 through to A.V.10 shows the comparison of the machine torque/speed characteristic for the machine supplied on PWM and same machine predicted characteristic for selected frequencies.

Figure A.V.1 shows three torque/speed characteristics. These are machine supplied on PWM, same machine supplied at pure AC and predicted with supplied on pure AC and 220 Volt at 50 Hz. It is evident from these curves that the developed machine torque for a given value of slip is available on PWM is virtually the same as that available on pure AC. However, the torque at 0.943 of slip on PWM is approximately 24% lower than on 220 Volt pure AC and predicted. As suggested by (Besanov,1991), according to Jain(1964), the presence of harmonics in the supply voltage waveform would result in a reduction in machine torque at any given slip. It is also suggested by TeqQuipment.

The induction motor is also simulated at 50 Hz and 200 Volt, as the actual output voltage of the PWM supply is 200 Volt. The predicted torque/speed curve at 200 Volt pure AC and PWM torque/speed curve are seen from figure A.V.2. In this figure, the predicted torque/speed curve matches better to PWM torque/speed curve, because of, actual output voltage of the PWM supply is 200 Volt. At 0.943 of slip on PWM is approximately 3% lower than on predicted 200 Volt pure AC. Even from 0.98 of slip to 0.95, PWM torque is higher than predicted torque about 10% in spite of the presence of harmonics.

Machine performance characteristics are presented for operating frequency of 40 Hz, 30 Hz, 20 Hz and 10 Hz PWM supply, and the results are shown in figure A.V.3 thorough to figure A.V.6. Refer to figure A.V.3, which depicts machine torque/speed characteristic at 40 Hz PWM supply, shows that maximum available torque is approximately 4.5 Nm and occurs at the relative slip value of 0.937 and predicted torque values is about 4.9 Nm at this relative slip. It is also seen from this figure that the PWM developed machine torque for a given value of slip is virtually same with predicted torque, although the PWM results are a little lower than predicted values. Because of the harmonic content and insufficient output voltage of the inverter, the resulting PWM torque values may have been lower than the predicted values. The inverter output voltage was measured as 156 Volt, while it should be about 176 Volt.

Figure A.V.4, which depicts machine torque/speed characteristic at 30 Hz PWM supply, shows that maximum available test torque is again approximately 4.5 Nm and occurs at the relative slip value of 0.90, and predicted torque value is about 5.5 Nm at this relative slip. It is also seen from this figure that the PWM developed machine torque for a given value of slip is virtually same with predicted torque, although PWM results are approximately 20% lower than the predicted values. Here the same argument which is presented above for 40 Hz is acceptable and also supported. The inverter output voltage was measured as 120 Volt, while it should be about 132 Volt.

The machine torque/speed characteristic at 20 Hz PWM supply is seen from figure A.V.5. Maximum available torque is 4.5 Nm for PWM source and occurs at the relative slip value of 0.875 and the predicted torque value is about 4.5 Nm at this relative slip. It is also seen from this figure that the PWM developed machine torque for a given value of slip is much the same as the predicted torque.

Figure A.V.6, which depicts machine torque/speed characteristic at 10 Hz PWM supply, shows that maximum available torque is again approximately 4.5 Nm and occurs at the relative slip value of 0.716, and the predicted torque value is about 4 Nm at this relative slip. It is also seen from this figure that the PWM developed machine torque for a given value of slip is virtually same as the predicted torque, even PWM results are approximately 20% higher than predicted values. This indicates the likelihood of extra boost voltage. In low frequencies to provide demanded torque, the boost voltage has to be applied at this frequency. The inverter output voltage was measured as 48 Volt, while it should be about 44 Volt.

It is noted that maximum torque occurs at larger slip for lower frequencies. It is known from induction motor machine theory(Bezanov,1991), (Bose(a),1986), (Chapman,2002) that maximum (or transition) slip is the ratio of the rotor resistance to the stator leakage reactance. It is therefore expected and monitored for variable frequency operations. So these qualitative observations suggest that the machine is behaving as expected under variable supply frequencies.

Operation above 50 Hz was investigated for operating frequencies of 60 Hz, 70 Hz, 80 Hz and 90 Hz. Resulting torque/speed curves, which the machine supplied at rated voltage and PWM supply and predicted pure AC torque/slip characteristics, are shown in figure A.V.7 thorough figure A.V.10. These figures indicates that maximum available torque values are at approximately 4.5 Nm, 3 Nm, 2.5 Nm and 1.7 Nm and these occur at relative slip values of 0.927 , 0.937 , 0.935 , 0.948 respectively. The predicted torque values are about 5.9 Nm, 4.1 Nm, 4.0 Nm, 2.9 Nm respectively, at these relative slip values. As mentioned before, in section 4.2, the maximum available predicted torque values are 13.42 Nm, 10.44 Nm, 8.35 Nm, 6.83 Nm respectively and this values occur at relative slip of 0.62 , 0.66., 0.7 and 0.73 respectively. This is the consistent with the previously mentioned relationship describing the transition slip in terms of rotor resistance and stator leakage reactance. At the higher frequencies the leakage reactance is increased and therefore the value of transition slip reduces. This means that relative slip is increased and it is also noted that the usable torque at higher operating frequencies is further reduced since friction and windage losses are increased. Additionally, it is clear from figure A.V.7 thorough figure A V.10 that resulting PWM torque values are approximately 20% lower than predicted torque values at any given relative slip values because of the high harmonic content due to high switching of SCRs of inverter to provide sinusoidal current waveforms.

5.3. Limitations of Operation

Load tests for all selected frequencies were done until current reached about 4.8 A, and all measurements were done until the machine current was about 4.5 A for safe operation. So, in all experimental work, maximum torque could not applied and the relative slip for maximum torque could not determined.

Additionally, usable torque at higher operating frequencies is further reduced since applied voltage was not increased(or maintained constant), and friction and windage losses are increased. Consequently load tests were implemented up to 90 Hz and not implemented for 100 Hz.

6. CONCLUSION

The performance of an induction motor over an acceptable frequency range and also its performance at the lower and higher ends of that range has been investigated. It has been demonstrated that when the induction motor is supplied by a PWM source at variable frequencies, the motor performance under load testing is compatible with its performance under sinusoidal excitation and computed also results.

When the induction motor was supplied by the PWM source at 50 Hz, torque/speed characteristic under load testing is compatible with a supply of conventional pure AC source at 50 Hz. However PWM results are lower about 20% than pure AC and computed results. This was expected, because as mentioned in section 5.2 output voltage of PWM source was measured about 200 Volt while it needed to be 220 Volt. Another factor is the high harmonic content of PWM waveform as mentioned in section 3.3.4.

The machine was load tested below the base frequency range by varying the supply frequency and maintaining the ratio V/f = constant, and its performance was determined. Although the resulting torque/speed curves for 30 Hz and 40 Hz are a little lower than computed results, it may be suggested that the resulting torque/speed curves are closed to the computed results, especially for 20 Hz, as the ratio V/f was exactly maintained by PWM source as it should be for this frequency. Here the same argument, presented above, about the harmonic content for 50 Hz is also acceptable. It may be said that if harmonic content of PWM inverter would be eliminated and the ratio V/f would be maintained exactly, the resulting torque/speed curves would be matched better to the computed results.

The machine was load tested above the base frequency range by varying the supply frequency and maintaining the voltage is constant, and its performance has been also demonstrated. It is evident from the results presented in chapter 5 that although the resulting torque/speed curves for 60, 70, 80 and 90 Hz are lower than the computed results, it may be however suggested that the resulting torque/speed curves are closed to the computed results. This is likelihood of the low voltage output of inverter and high harmonic content. Because, the inverter output voltage was measured as about 200 Volt, while it should be 220 Volt and it is evident from monitored harmonic results in section 3.3.4 that PWM waveform contains high harmonic content. So it may be said again that if harmonic content of PWM inverter would be eliminated and 220 Volt constant output voltage would be provided, the resulting torque/speed curves would be matched to the computed results for the region above 50 Hz.

Nevertheless, it may be concluded that the machine is behaving as expected under variable supply frequencies and it is seen from the figures, which are given in appendices III, that the output current waveform of inverter function as a sinusoid and the PWM inverter automatically regulates the energy it obtains to suit the load conditions.

An interesting development would be to design the induction motor for operation at higher frequencies, may up to 200 Hz. The operational constrains would be voltage level limits set by the insulation, and the mechanical maximum speed. Improvements in laminated sheet steels make this possible. The PWM source range would have to be extended with the addition of an extra DC level voltage, i.e. two or three DC voltage levels to give a wide range of quality volt/frequency control(Andersen, Horton and Cartwright, 2002), (Lafoz, Iglesias and Veganzones), (Sto, Green and Coonik, 1996).

An AC drive block diagram which is inverter supplied by three-level converter and one phase circuit diagram of three-level converter is shown in Appendices in figure A.VII.1 and figure A.VII.2 respectively. Converter section of AC drive systems has normally one DC output. But this DC output can be obtained in three-level as shown in figure 6.1 and 6.2 and inverter can be supplied by this DC voltage levels. By utilizing the multi-level converter topology; a concept whereby the converter allows more possibilities for the AC phase voltage levels than with a standard drive. The increase in voltage levels leads to lower semiconductor device switching frequency and thus lower switching losses.

REFERENCES

ANDERSEN, B. R., XU L., HORTON P. J., CARTWRİGHT P., 2002. Topologies for VSC Transmission, IEE Power Electronic Journal, Vol.16, No.3, 142-150.

BEZANOV, G., 1991. On-Line Control of Microprocessor-Based PWM for A.C. Drives, Brunel University, Ph. D. Thesis, England, 341p.

BOSE, B. K. (a), 1986. Power Electronics and AC Drives, USA, 402p.

___________(b), 1992. Recent Advanced in Power Electronics, IEEE Transactions on Power Electronics, Vol.7, No.1, 2-16.

___________(c), 2000. Energy, Environment, and Advances in Power Electronics, IEEE Transactions on Power Electronics, Vol.15, No.4, 688-701

BOSE, B. K., GRABOWSKI, P.Z., and KAZMIERKOWSKI, M.P, 2000. A Simple Direct-Torque Neuro-Fuzzy Control of PWM-Inverter-Fed Induction Motor Drive, IEEE Transactions on Industrial Electronics, Vol.47, No.4, 863-870

CHAPMAN, S.J., 2002. Electric Machinery and Power System Fundamentals. Ed. McGraw-Hill, Inc.Singapore, 673p.

CONKLING, D.A., 2000. Energy Efficient Motors and Adjustable Speed Drives, USA , 97p.

DRURY, W., Electrical Variable Speed Drives, Control Techniques plc, UK, http://www.drivesportal.com/technical_articles/pdf/electric.pdf

HUI, S.Y.R.,SATHIAKUMAR, S. and SUNG K.K., 1996. Novel Random PWM

Schemes With Weighted Switching Decision, Power Electronics and Variable Speed Drives Conference, 348-353.

KADANIK, P., 1998. Prague, http://kevf72.troja.mff.cuni.cz/xichty/lab7/ downloads/ reports/ac_drives_diagnostics.pdf

LAFOZ, M., IGLESIAS, I. J., VEGANZONES, C., Three-Level Voltage Source Inverter with Hysteresis-Band Current Control, Spain, http://www.cedex.es/ceta/cetaweb/info_fisicas/convertidor3n_epe01.pdf

LEESON ELECTRICAL CORPORATION, 1999. Basic Training Motors, Gears & Drives, USA, http://www.leeson.com/literature/tech_info/pdf/ basictraining.pdf

LEWIS, E.A., 1996. Cycloconvertor Drive Systems, Power Electronics and Variable Speed Drives Conference, 383-389.

MELFI, M. J., AC Induction Motors as Part of Variable Speed Drive Systems, Rockwell Automation, USA , http://www.reliance.com/pdf_elements/ b7113.pdf

MIHOUB, Y., MAZARİ. B., FASLA, S., 2001. Neuro-Fuzzy controller used to Control of An Induction Motor, Second International Conference on Electrical and Electronics Engineering, 83-87.

MOHADDES, M., 1998. Control Of Optimal Pwm Voltage Source Inverter Using Sigmoid And Picewise Linear Artificial Neural Networks, Proceedings of the 1998 Graduate Student Conference, GRADCON'98, Canada, http://www.ee.umanitoba.ca /~gradcon/gradcon98/proceed

OZPINECI, B. And TOLBERT, L.M.,Cycloconverters, USA, http://www.pels.org/Comm/Education/Tutorials/cycloconvertertutorial.pdf

RAMSHAW, R. S., Power Electronics Semiconductor Switches, Chapman and Hall, England, 458p.

RICHARDSON, J., BEZANOV, G.J. And HASHEM ,G.M., 1996. Optimal PWM Waveform Modelling for On-Line AC Drive Control, Power Electronics and Variable Speed Drives Conference, 496-501.

SETHURAMAN,S. K. and SARAVAN M.M., 1994. Pulse Width Modulated Embedded Control and On-Line Condition Monitoring of Induction Motors, Proceedings of the 29th Universities Power Engineering Conference, 645-648.

SIEMENS, Micromaster and Midimaster Manuel, acdrives2.pdf

STO,D., GREEN, T.C. and COONIK A., 1996. Multi-Level Converters and Large Power Inverters, Power Electronics and Variable Speed Drives Conference publication No. 429, 354-359.

TECQUIPMENT LIMITED (a), MPM1015 Variable Frequency Inverter Drive Manuel

________________________ (b), NE7010 Electrical Machines Test Bench Manuel

BIOGRAPHY

I was born in Adana, January 19^{th} , 1969. I graduated from high school in 1985 and one year later, in 1986, I entered to Electrical and Electronics Engineering of Dokuz Eylül University in İzmir. I received my B.S. Degree in 1990. After completing my Military Service in 1992, I began to work in AKSANTAŞ Textile Factory as Electrical and Electronics Engineer. In 1995, I was assigned to Industrial and Medical Electronic Research and Application Center in Çukurova University. Then, I was assigned to Balcalı Hospital in Çukurova University in April 2002. I have been still working there at same position.

APPENDICES

A.I. AC Motor Parameters

Sno	Parameters	Quantity	Unit
DC test for stator resistance			
1	V_{dc}	50	Volt
2	I_{dc}	6	Ampere
3	R_{dc}	7,3	Ohm
4	$R_{ac} = R_s$	8,03	Ohm
(NL) No-Load test			
5	V at No-Load	223	Volt
6	P_{in} at No-Load total	240	Watt
7	P_{in} at No-Load phase	80	Watt
8	I at No-Load	3,4	Ampere
9	I_{Line} (dividing I to sqrt(3))	1,963	Ampere
(LR) Locked Rotor Test			
10	V at Locked Rotor	58,3	Volt
11	P at Locked Rotor	116	Watt
12	I at Locked Rotor	2,8	Ampere
13	(P_{scl}) Stator copper loss	30,942	Watt
14	Core and Rotation loss	49,057	Watt
15	Locked Rotor impedance($Z_{LR}= V_{BL} / I_{BL}$)	20,821	Ohm
16	Cosφ (P_{in} =Sqrt(3)xV_{BL} x I_{Bl} x Cos φ)	0,4102	Watt
17	φ	1,1480	Radian
18	R_{LR} ($R_{LR} = Z_{LR}$ x Cosφ)	8,5424	Ohm
19	R_r ($R_s + R_r = R_{LR}$ so $R_r = R_{LR} - R_s$)	0,5124	Ohm
20	X_{LR} ($X_{LR} = Z_{LR}$ x Sinφ)	18,988	Ohm
21	X_s ($X_s = X_r = X_{LR} / 2$)	9,4941	Ohm
22	Xr (Xs = Xr = XLR / 2)	9,4941	Ohm
23	Z_{NL} ($V_{NL} / I_{NL} = X_s + X_m$)	113,602	Ohm
24	$X_m = (Z_{NL} – X_s)$	104,108	Ohm

A.II. PWM Experimental Test Resulting Torque/Speed Curves

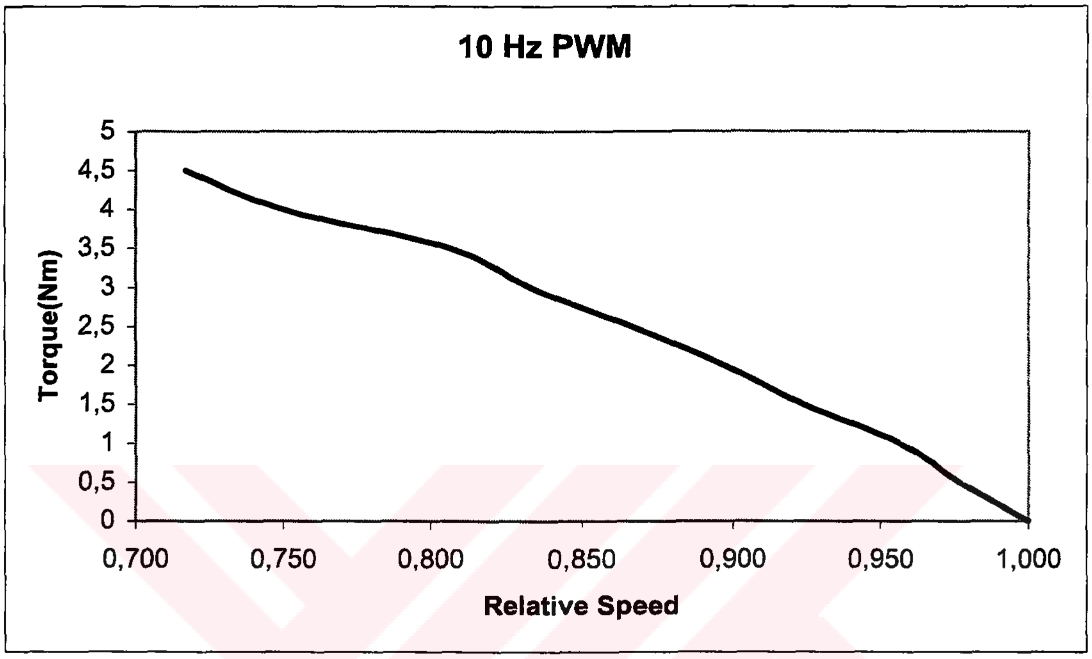

Figure A.II.1 Torque/speed curve f=10 Hz (PWM)

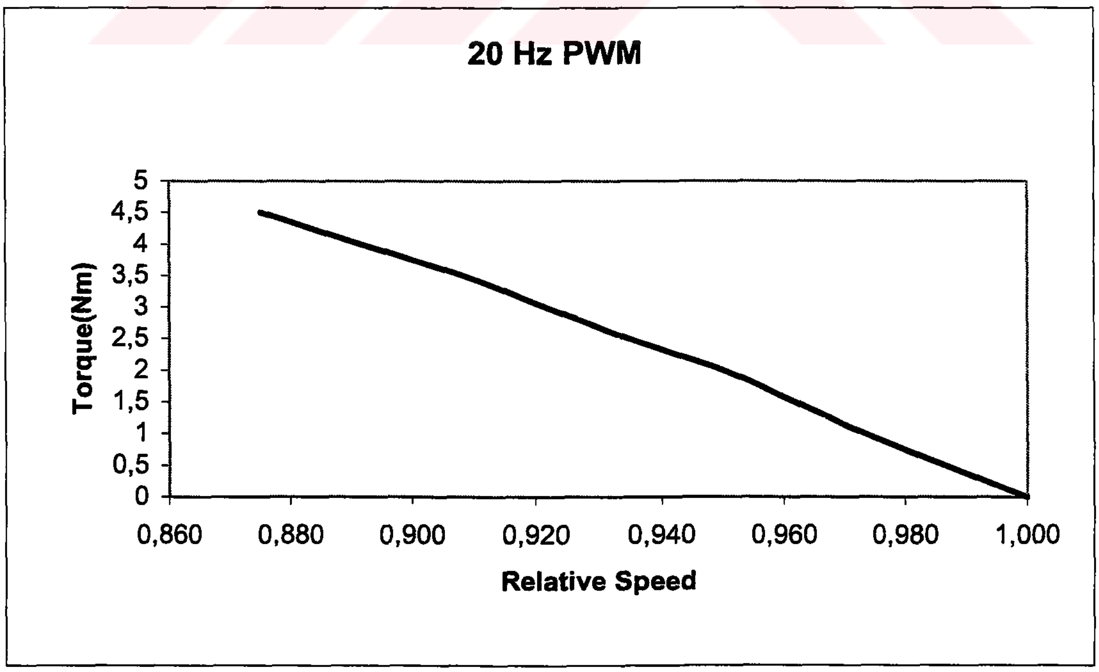

Figure A.II.2 Torque/speed curve f=20 Hz (PWM)

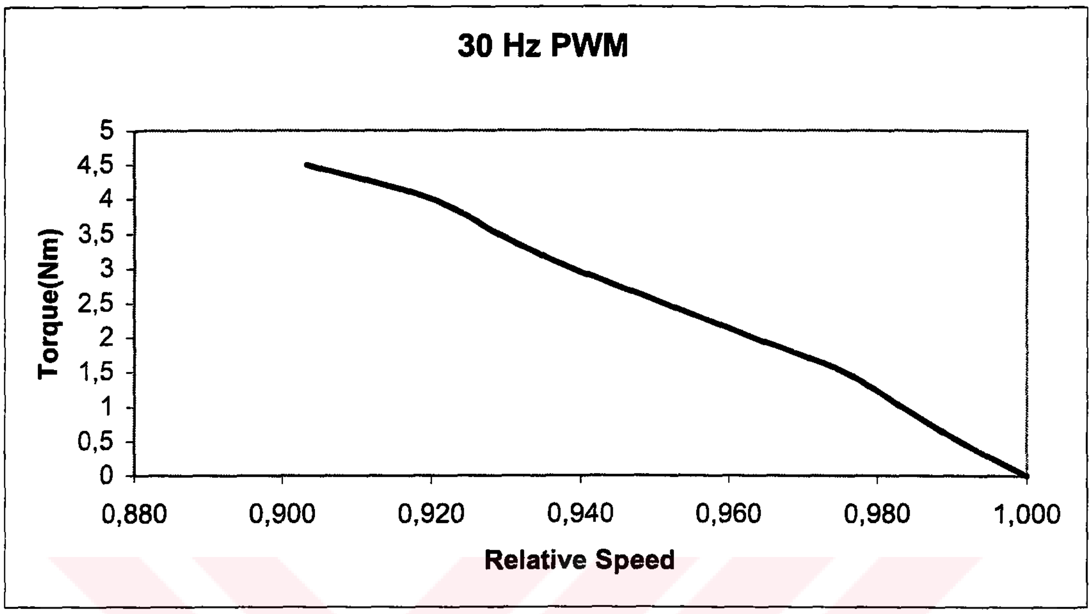

Figure A.II.3 Torque/speed curve f=30 Hz (PWM)

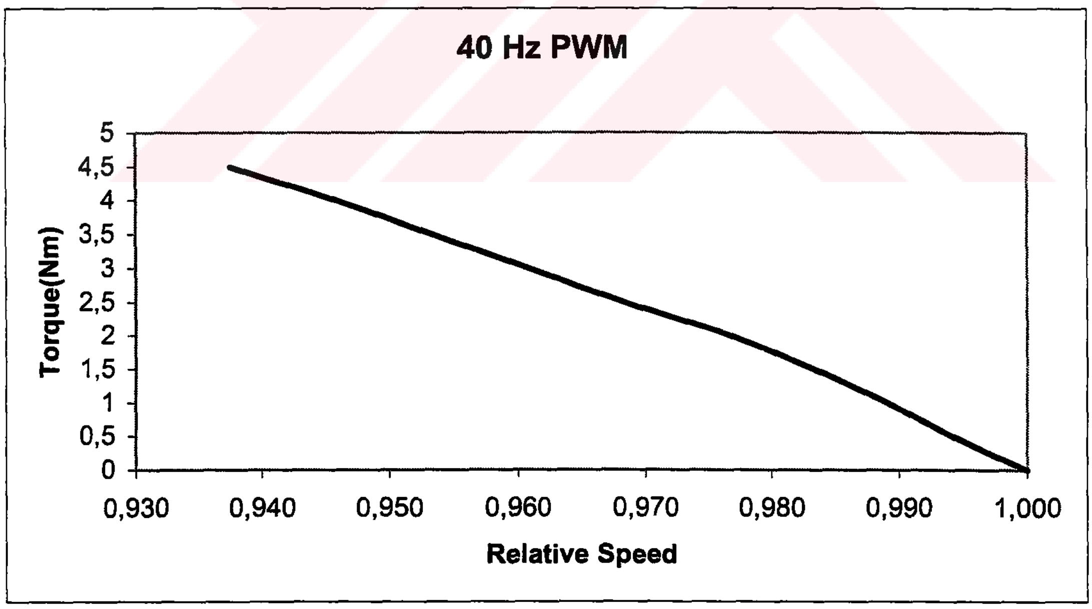

Figure A.II.4 Torque/speed curve f=40 Hz (PWM)

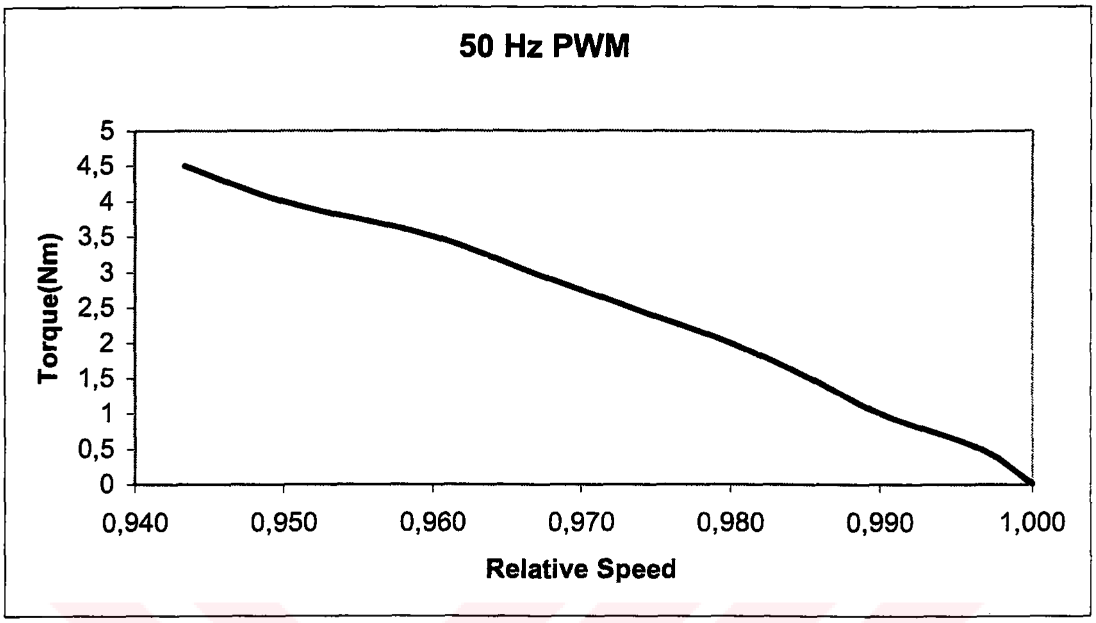

Figure A.II.5 Torque/speed curve f=50 Hz (PWM)

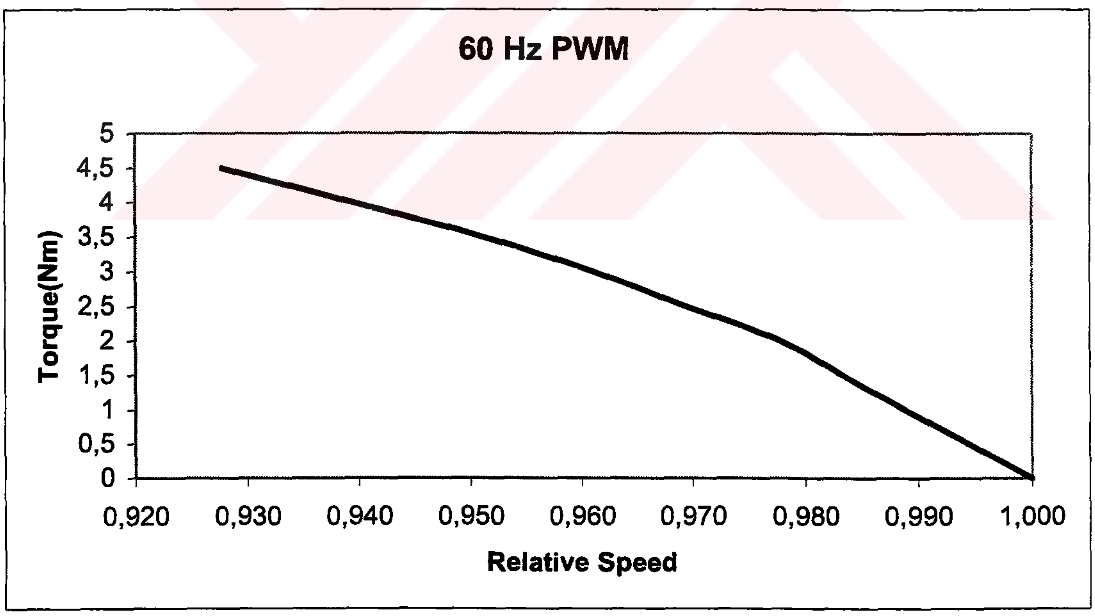

Figure A.II.6 Torque/speed curve f=60 Hz (PWM)

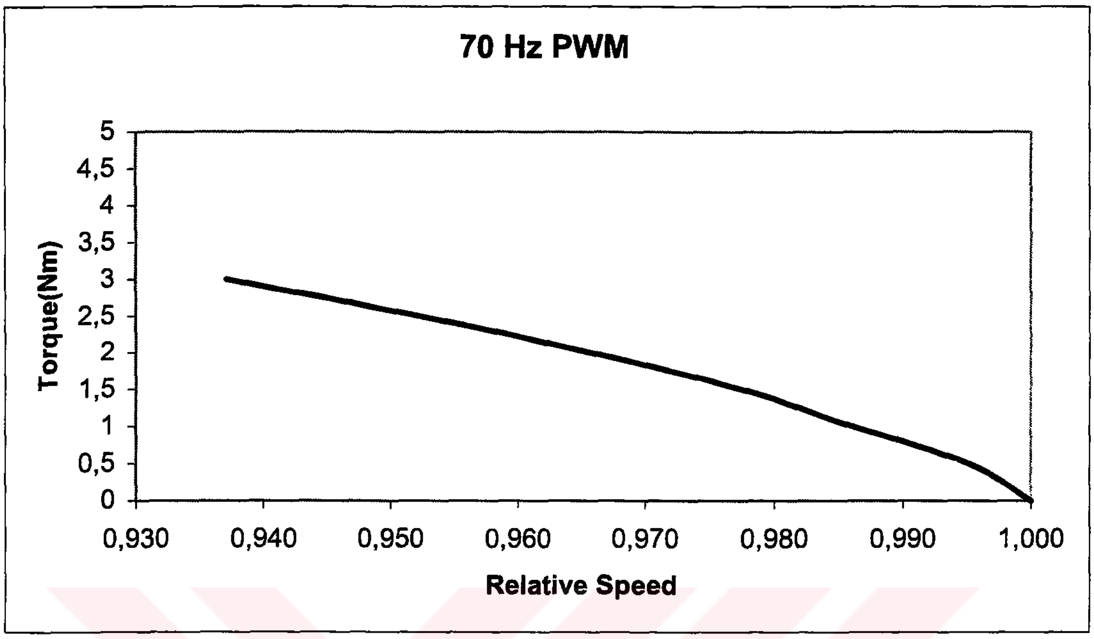

Figure A.II.7 Torque/speed curve f=70 Hz (PWM)

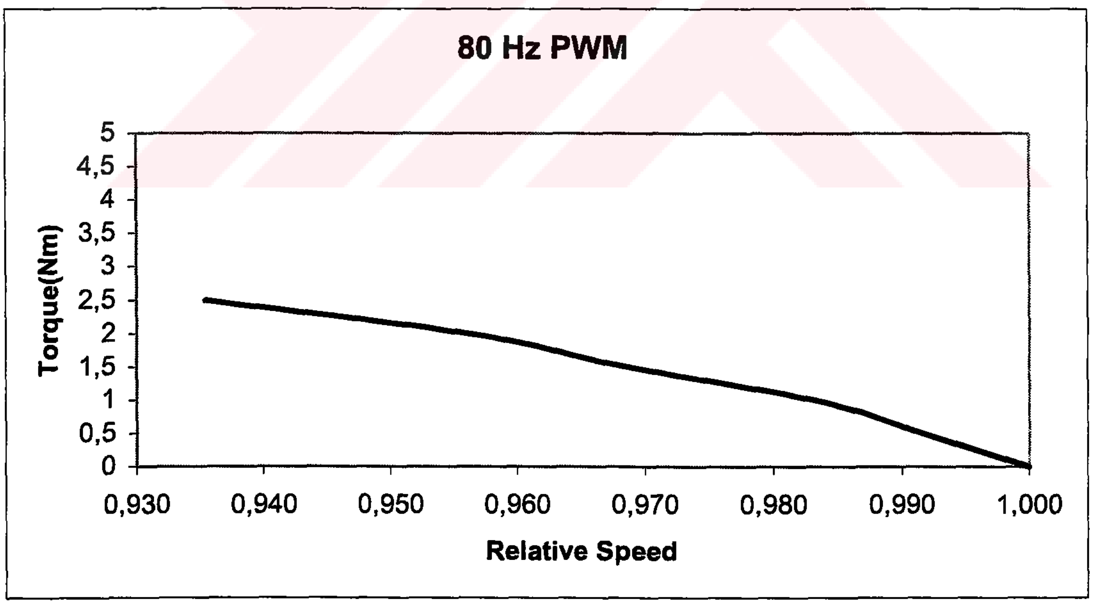

Figure A.II.8 Torque/speed curve f=80 Hz (PWM)

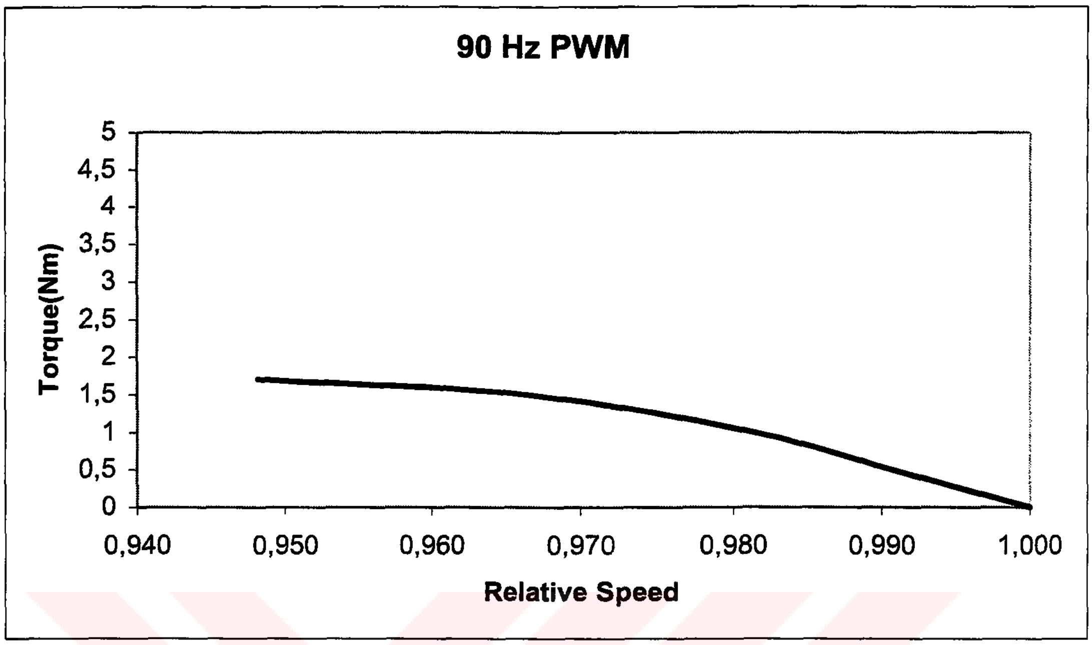

Figure A.II.9 Torque/speed curve f=90 Hz (PWM)

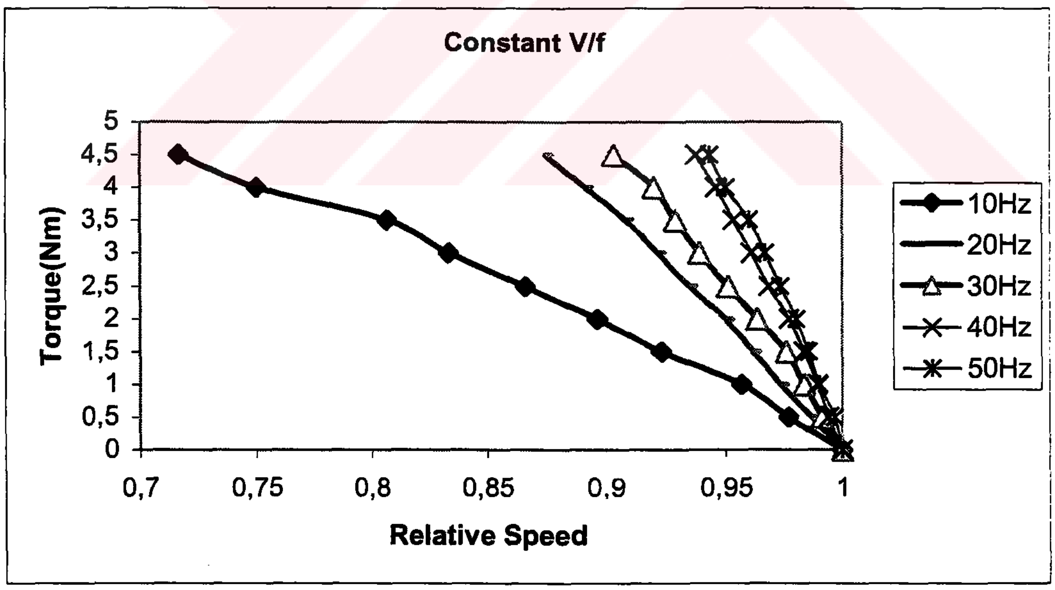

Figure A.II.10 Torque/speed curve at Constant V/f (PWM)

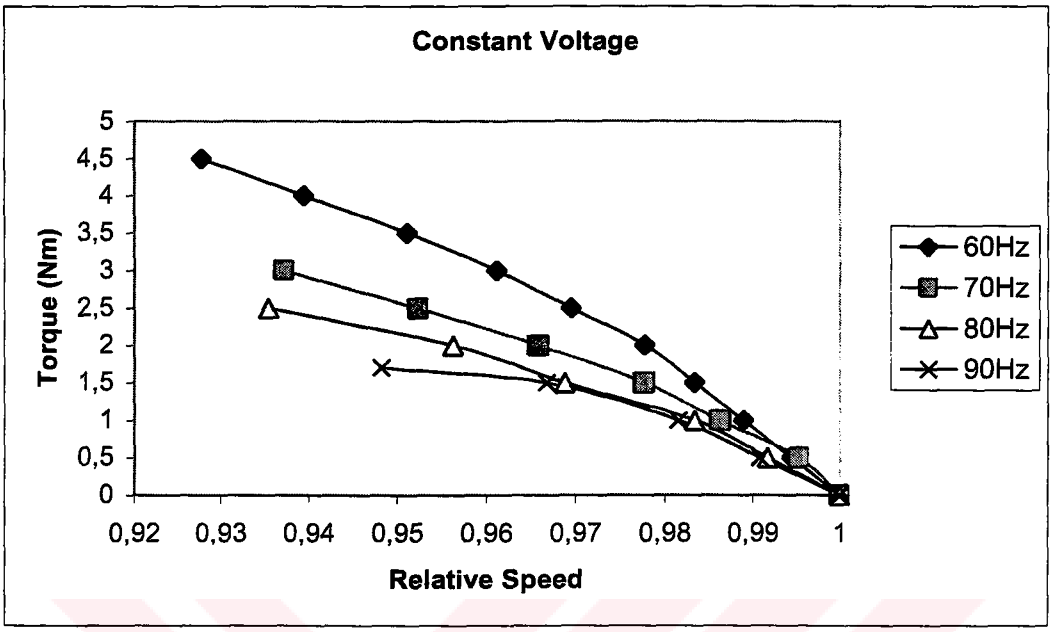

Figure A.II.11 Torque/speed curve at Constant Voltage (PWM)

A.III. PWM Voltage an Current Waveforms

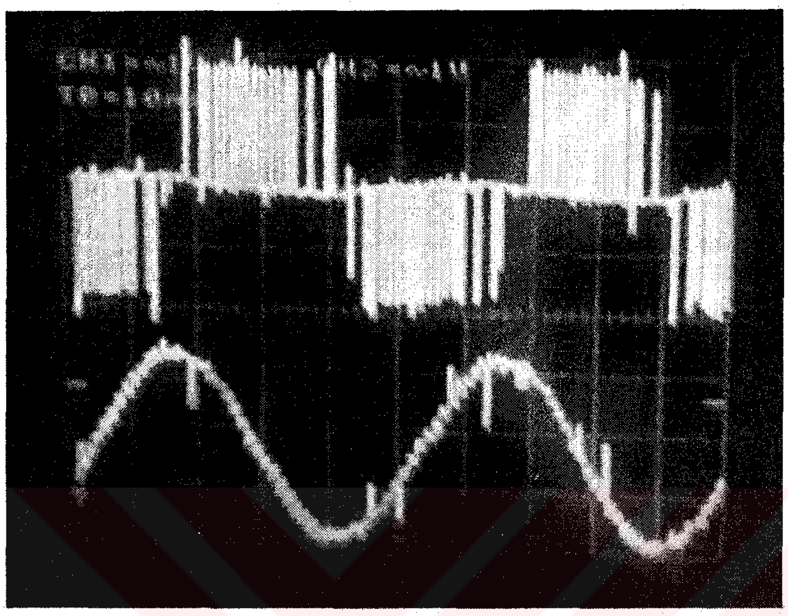

Ch_1 = 1 Volt, Ch_2= 1 Volt, Time/Div = 10 ms

Figure A.III.1 Voltage and Current waveform at f=20 Hz and T= 0 Nm

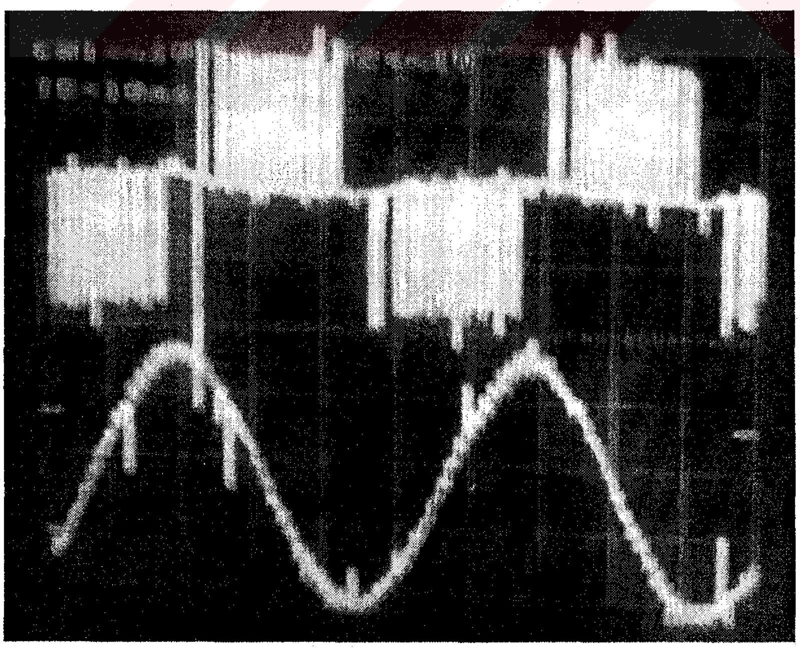

Ch_1 = 1 Volt, Ch_2= 1 Volt, Time/Div = 10 ms

Figure A.III.2 Voltage and Current waveform at f=20 Hz and T= 3 Nm

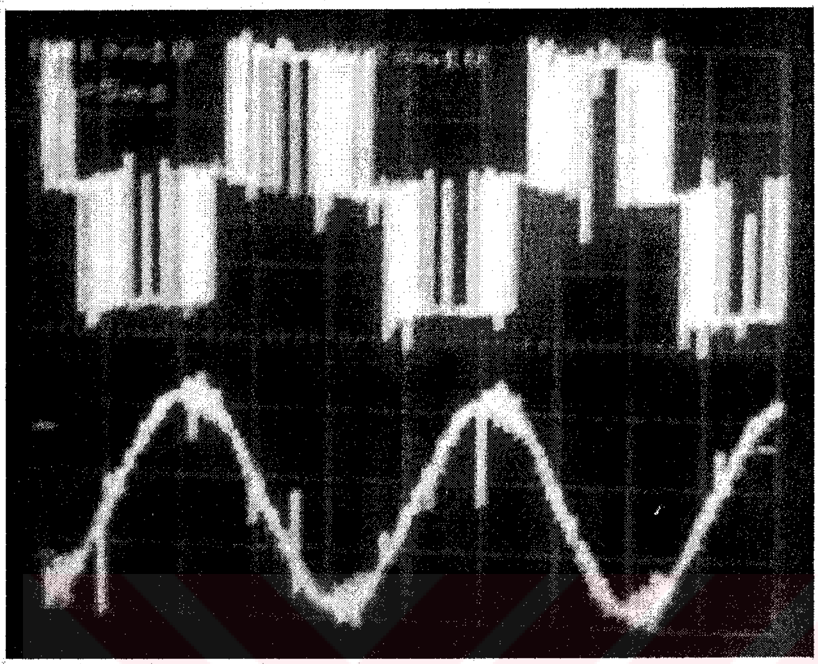

Ch_1 = 1 Volt, Ch_2 = 1 Volt, Time/Div = 5 ms

Figure A.III.3 Voltage and Current waveform at f=50 Hz and T= 0 Nm

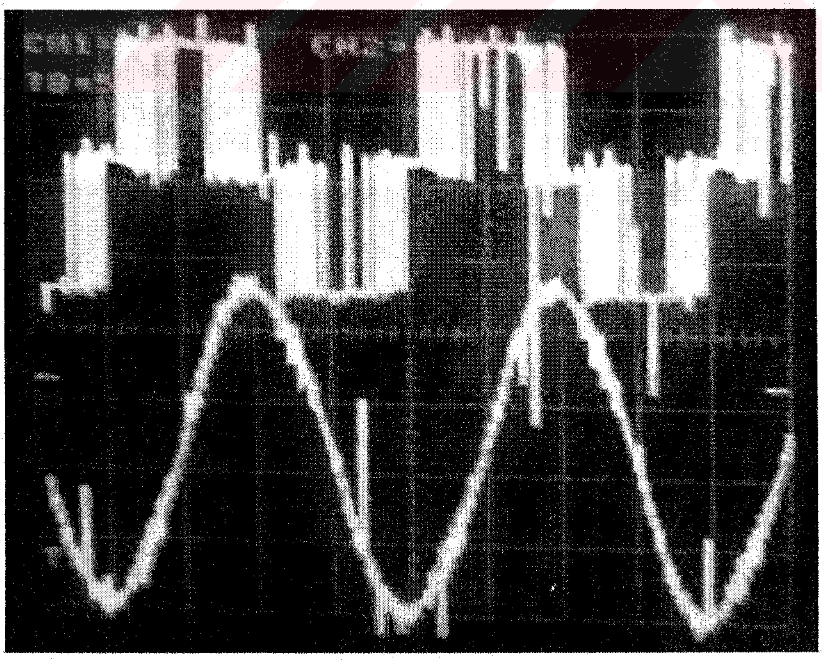

Ch_1 = 1 Volt, Ch_2 = 1 Volt, Time/Div = 5 ms

Figure A.III.4 Voltage and Current waveform at f=50 Hz and T= 4 Nm

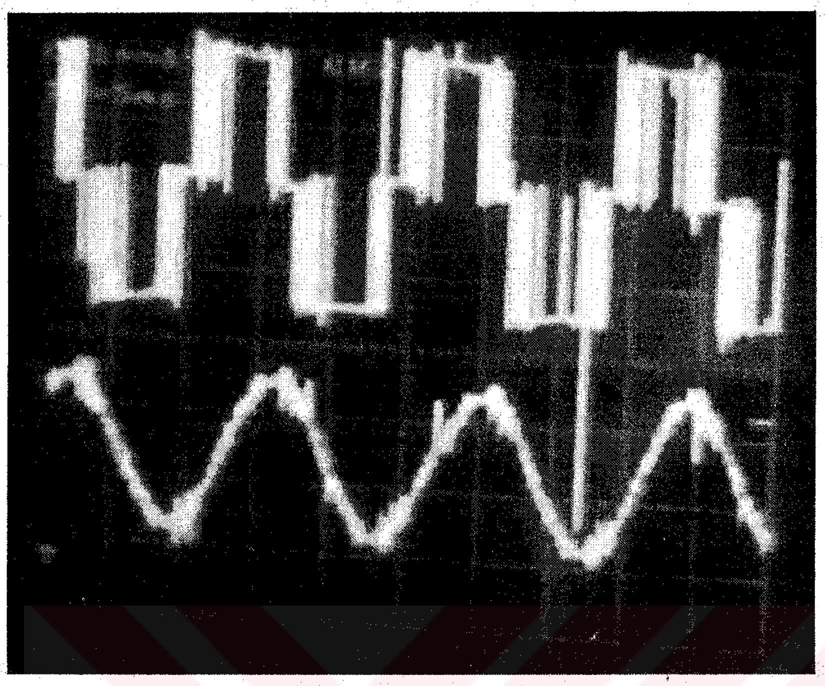

Ch$_1$ = 1 Volt, Ch$_2$= 1 Volt, Time/Div = 5 ms

Figure A.III.5 Voltage and Current waveform at f=70 Hz and T= 0 Nm

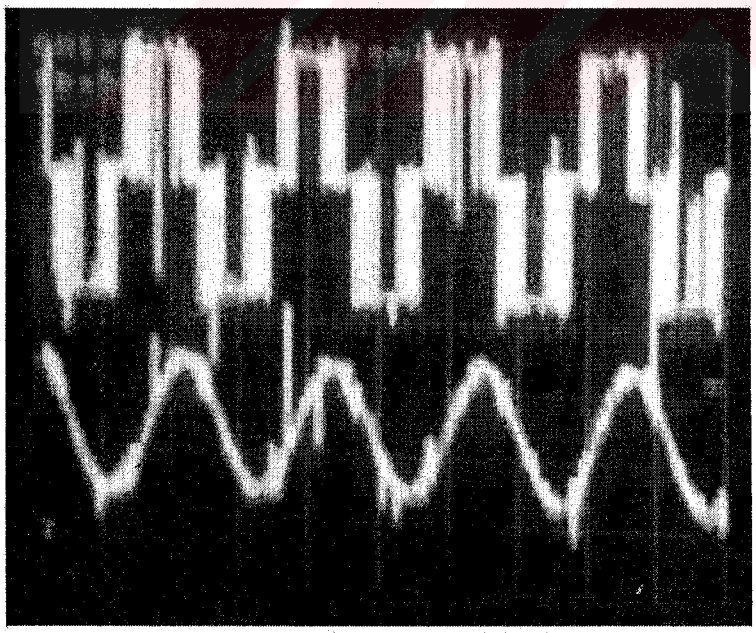

Ch$_1$ = 1 Volt, Ch$_2$= 1 Volt, Time/Div = 5 ms

Figure A.III.6 Voltage and Current waveform at f=90 Hz and T= 0 Nm

A.IV. Computer Programs

A-IV.I. Induction Motor Constant V/f Simulation Source Code

```
/**********************   CONSVF.CPP   ******************/

/* gives data for torque-speed curves at constant Volt/hertz */

#include <stdio.h>
#include <conio.h>
#include <stdlib.h>
#include <math.h>
void main()
{
      FILE *di, *di3;     /* to write output datas a file */

/*** INPUT EQUIVALENT CIRCUIT PARAMETERS  *****/

      float Rs=8.03, Rr=7.24, Xs50Hz=7.3248, Xs, Ls, Xr50Hz=7.3248,
Xr, Lr, Xm50Hz=104.364, Xm, Lm, VLine_constant=220.0, VLine;
      float frekans, Ns, ws, Smax,torque_constant,Pole=4.0;

/* Define Strings for Outputs */

      float  Xf[250], Xt[250], Zt[250], Rf[250], Rt[250], R[250],
den[250], fi[250], wr[250], Pag[250], Pt[250], Tt[250], pf[250] ;
      float  Xfx[250], Xtx[250], Ztx[250], Rfx[250], Rtx[250],
denx[250], Pagx[250], Ptx[250], Tth[250], Ttx[250],
eff[250],fit[250],pft[250];
      float  Is[250], Ir[250], loss[250];


      printf("*** INPUT EQUIVALENT CIRCUIT PARAMETERS  ***\n");
      printf(" Plesa Input Frequency :   ");
      scanf("%f",&frekans);


      torque_constant=VLine_constant/(2.0*3.14*50.0);
      VLine=torque_constant*2.0*3.14*frekans;

/*    Calculating Reactance in Input Frequency ******/

      Ls=Xs50Hz/(2.0*3.14*50.0);
      Lr=Xr50Hz/(2.0*3.14*50.0);
      Lm=Xm50Hz/(2.0*3.14*50.0);

      Xs=Ls*2.0*3.14*frekans;
      Xr=Lr*2.0*3.14*frekans;
      Xm=Lm*2.0*3.14*frekans;

/*    End of Calculating */

      Ns=(120.0*frekans)/Pole;
```

```
	ws=Ns*2.0*3.14/60.0;
	Lr= Xr/(2.0*3.14*50.0);
	Smax=(Rr/Lr)/ws;
	printf(" Freq.=%f Ns=%f ws=%f t.Cons.=%f VLine=%f \n
",frekans,Ns,ws,torque_constant,VLine);

	int i ;
	float X, XX, Vph, Vth, slip, s=0.0 ;
	Vph=VLine;
	X = (Xr+Xm);
	XX = (Xs+Xm);
	Vth=Vph*(Xm/XX);

	printf(" Vph = %f and Vth = %f  \n ",Vph,Vth);
	printf(" Xs  = %f Xr = %f            Xm = %f \n ",Xs,Xr,Xm);

/* Opening Files in Writing Mode */

	if((di=fopen("c:\\tez\\emachine\\xls\\50_less\\cvf.txt","w"))
== NULL)
		{
		printf(" Consvf.TXT FILE COULDN'T BE OPENED !!!\n");
		exit(0);
		}
	fprintf(di, "frekans    s     slip  Pt    Tt    Is    pf
	Vph=VLine   VLine_constant \n  ");

	if((di3=fopen("c:\\tez\\emachine\\xls\\50_less\\cvf_tv.txt","w
")) == NULL)
		{
		printf(" Consvftv.TXT FILE COULDN'T BE OPENED !!!\n");
		exit(0);
		}
	fprintf(di3, "frekans    s     slip  Ptx   Ttx   Ir    pf
	V_Thevenin  VLine_constant \n  ");


	for(i=0; i<100;i++)
	{
	s=s+0.01;

/*******************************************/
/*    Normal Equivalent Circuit          */
/*******************************************/

	R[i]=Rr/s;
	den[i]=( R[i]*R[i] + X*X );
	Rf[i]=( R[i]*Xm*Xm )/den[i];
	Xf[i]=( R[i]*R[i]*Xm + (Xr*Xm)*X )/den[i];
	Rt[i]= Rs + Rf[i];
	Xt[i]= Xs + Xf[i];
	Zt[i]= sqrt(Xt[i]*Xt[i] + Rt[i]*Rt[i]);
	fi[i]= atan(Xt[i]/Rt[i]);
	pf[i]= cos(fi[i]);
	wr[i]= (1.0-s)*ws;
	Is[i]= Vph/Zt[i];
```

```
      Pag[i]= 3.0*( Is[i]*Is[i] )*Rf[i];
      Pt[i]=((1.0-s)*Pag[i])  ;
      Tt[i]= Pt[i]/wr[i];

      loss[i]= s*Pag[i] + 3.0*Is[i]*Is[i]*Rs;
      eff[i]= 100.0*(1.0 - (loss[i] / (loss[i]+Pt[i])));

/******************************************/
/*    Thevenin Parameter Calculation    */
/******************************************/

      R[i]= Rr/s;
      denx[i]=( Rs*Rs +XX*XX );
      Rfx[i]=( Rs*Xm*Xm )/denx[i];
      Xfx[i]=( Rs*Rs*Xm + (Xs*Xm)*XX )/denx[i];
      Rtx[i]= R[i] + Rfx[i];
      Xtx[i]= Xr + Xfx[i];
      Ztx[i]= sqrt(Xtx[i]*Xtx[i] + Rtx[i]*Rtx[i]);

      fit[i]= atan(Xt[i]/Rt[i]);
      pft[i]= cos(fi[i]);

      Vth= Vph*(Xm/XX);
      Ir[i]= Vth/Ztx[i];
      Ttx[i]= 3.0*Ir[i]*Ir[i]*R[i]/ws;
      Pagx[i]= 3.0*Ir[i]*Ir[i]*R[i];
      Ptx[i]= (1.0-s)*Pag[i];
      slip= (1.0-s);


       fprintf(di, "%f  %f    %f    %f    %f    %f    %f    %f    %f
\n  ",frekans,s,slip,Pt[i],Tt[i],Is[i],pf[i],Vph,VLine_constant);

       fprintf(di3,"%f  %f    %f    %f    %f    %f    %f    %f    %f
\n  ",frekans,s,slip,Ptx[i],Ttx[i],Ir[i],pft[i],Vth,VLine_constant);


      }/*  end of FOR Loop */

      fclose(di);

      fclose(di3);
      printf("PLEASE LOOK AT THE TXT FILES !!! ");
      getch();

}/*  end of void main function */
```

A-IV.II. Induction Motor Constant V/f Simulation Source Code

```
/**********************    VSABIT.CPP    ******************/

/* gives data for torque-speed curves at constant Volt Variable f */

#include <stdio.h>
#include <conio.h>
#include <stdlib.h>
#include <math.h>
void main()
{
      FILE *di, *di3;    /* to write output datas a file */

/*** INPUT EQUIVALENT CIRCUIT PARAMETERS  *****/

      float Rs=8.03, Rr=7.24, Xs50Hz=7.3248, Xs, Ls, Xr50Hz=7.3248,
Xr, Lr, Xm50Hz=104.364, Xm, Lm, VLine=220.0;
      float frekans, Ns, ws, Smax,torque_constant,Pole=4.0;

/* Define strings for outputs */

      float  Xf[250], Xt[250], Zt[250], Rf[250], Rt[250], R[250],
den[250], fi[250], wr[250], Pag[250], Pt[250], Tt[250], pf[250] ;
      float  Xfx[250], Xtx[250], Ztx[250], Rfx[250], Rtx[250],
denx[250], Pagx[250], Ptx[250], Tth[250], Ttx[250],
eff[250],fit[250],pft[250];
      float  Is[250], Ir[250], loss[250];

      printf("*** INPUT EQUIVALENT CIRCUIT PARAMETERS  ***\n");
      printf(" Please Input Frequency :    ");
      scanf("%f",&frekans);

/*    Calculating Reactance in Input Frequency ******/

      Ls=Xs50Hz/(2.0*3.14*50.0);
      Lr=Xr50Hz/(2.0*3.14*50.0);
      Lm=Xm50Hz/(2.0*3.14*50.0);

      Xs=Ls*2.0*3.14*frekans;
      Xr=Lr*2.0*3.14*frekans;
      Xm=Lm*2.0*3.14*frekans;

/*    End of Calculating */

      Ns=(120.0*frekans)/Pole;
      ws=Ns*2.0*3.14/60.0;
      Lr= Xr/(2.0*3.14*50.0);

      printf(" Freq.=%f Ns=%f ws=%f t.Cons.=%f VLine=%f \n
",frekans,Ns,ws,torque_constant,VLine);

      int i ;
      float X, XX, Vph, Vth, slip, s=0.0  ;
      Vph=VLine;
```

```
    X = (Xr+Xm);
    XX = (Xs+Xm);
    Vth=Vph*(Xm/XX);

    printf(" Vph = %f and Vth = %f  \n ",Vph,Vth);
    printf(" Xs  = %f Xr = %f            Xm = %f \n ",Xs,Xr,Xm);

/* Opening Txt files in Write Mode*/

    if((di=fopen("c:\\tez\\emachine\\xls\\50_big\\Vsabit.txt","w")
) == NULL)
          {
          printf(" Vsabit.TXT FILE COULDN'T BE OPENED !!!\n");
          exit(0);
          }
    fprintf(di, "frekans   s     slip  Pt    Tt    Is    pf
    VLine \n  ");


    if((di3=fopen("c:\\tez\\emachine\\xls\\50_big\\Vsab_tv.txt","w
")) == NULL)
          {
          printf(" Vsabittv.TXT FILE COULDN'T BE OPENED !!!\n");
          exit(0);
          }
    fprintf(di3, "frekans   s     slip  Ptx   Ttx   Ir    pf
    V_Thevenin \n  ");


    for(i=0; i<100;i++)
    {
    s=s+0.01;

/*******************************************/
/*    Normal Equivalent Circuit          */
/*******************************************/

    R[i]=Rr/s;
    den[i]=( R[i]*R[i] + X*X );
    Rf[i]=( R[i]*Xm*Xm )/den[i];
    Xf[i]=( R[i]*R[i]*Xm + (Xr*Xm)*X )/den[i];
    Rt[i]= Rs + Rf[i];
    Xt[i]= Xs + Xf[i];
    Zt[i]= sqrt(Xt[i]*Xt[i] + Rt[i]*Rt[i]);
    fi[i]= atan(Xt[i]/Rt[i]);
    pf[i]= cos(fi[i]);
    wr[i]= (1.0-s)*ws;
    Is[i]= Vph/Zt[i];
    Pag[i]= 3.0*( Is[i]*Is[i] )*Rf[i];
    Pt[i]=((1.0-s)*Pag[i])  ;
    Tt[i]= Pt[i]/wr[i];

    loss[i]= s*Pag[i] +  3.0*Is[i]*Is[i]*Rs;
    eff[i]= 100.0*(1.0 - (loss[i] / (loss[i]+Pt[i])));

/*******************************************/
```

```
/*    Thevenin Parameter Calculation    */
/*******************************************/

      R[i]= Rr/s;
      denx[i]=( Rs*Rs +XX*XX );
      Rfx[i]=( Rs*Xm*Xm )/denx[i];
      Xfx[i]=( Rs*Rs*Xm + (Xs*Xm)*XX )/denx[i];
      Rtx[i]= R[i] + Rfx[i];
      Xtx[i]= Xr + Xfx[i];
      Ztx[i]= sqrt(Xtx[i]*Xtx[i] + Rtx[i]*Rtx[i]);

      fit[i]= atan(Xt[i]/Rt[i]);
      pft[i]= cos(fi[i]);

      Vth= Vph*(Xm/XX);
      Ir[i]= Vth/Ztx[i];
      Ttx[i]= 3.0*Ir[i]*Ir[i]*R[i]/ws;
      Pagx[i]= 3.0*Ir[i]*Ir[i]*R[i];
      Ptx[i]= (1.0-s)*Pag[i];
      slip= (1.0-s);


       fprintf(di, "%f  %f    %f    %f    %f    %f    %f    %f  \n
",frekans,s,slip,Pt[i],Tt[i],Is[i],pf[i],Vph);

       fprintf(di3,"%f  %f    %f    %f    %f    %f    %f    %f  \n
",frekans,s,slip,Ptx[i],Ttx[i],Ir[i],pft[i],Vth);

      }/*  end of FOR Loop */

      fclose(di);

      fclose(di3);
      printf("PLEASE LOOK AT THE VSABIT FILES !!! ");
      getch();

}/*  end of void main function */
```

A.V. PWM and AC Source Torque/Speed Curves

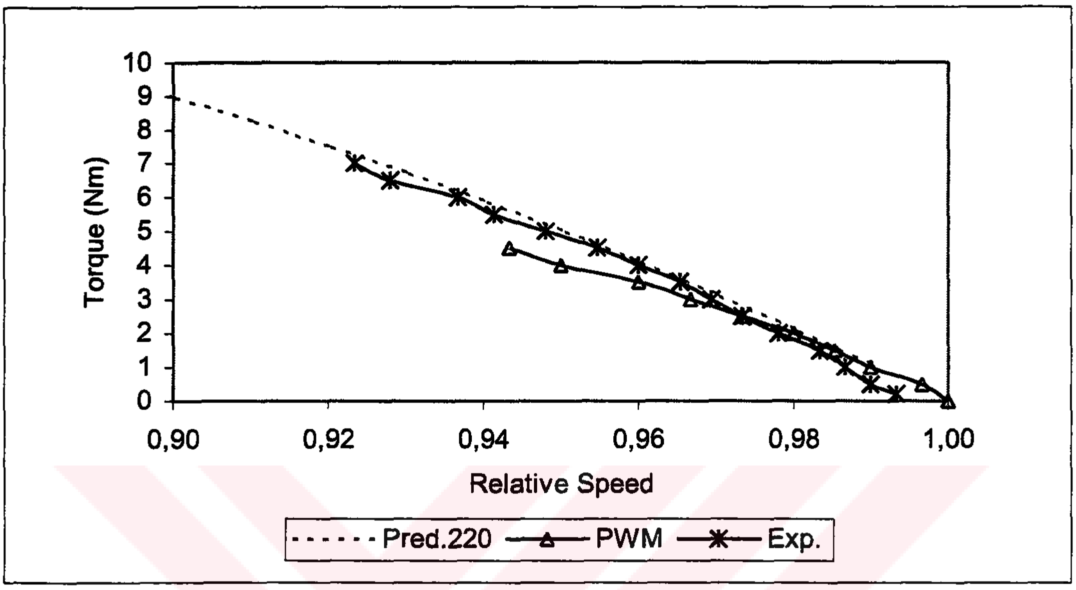

Figure A.V.1 Torque/speed curve at V=220 Volt, f=50 Hz

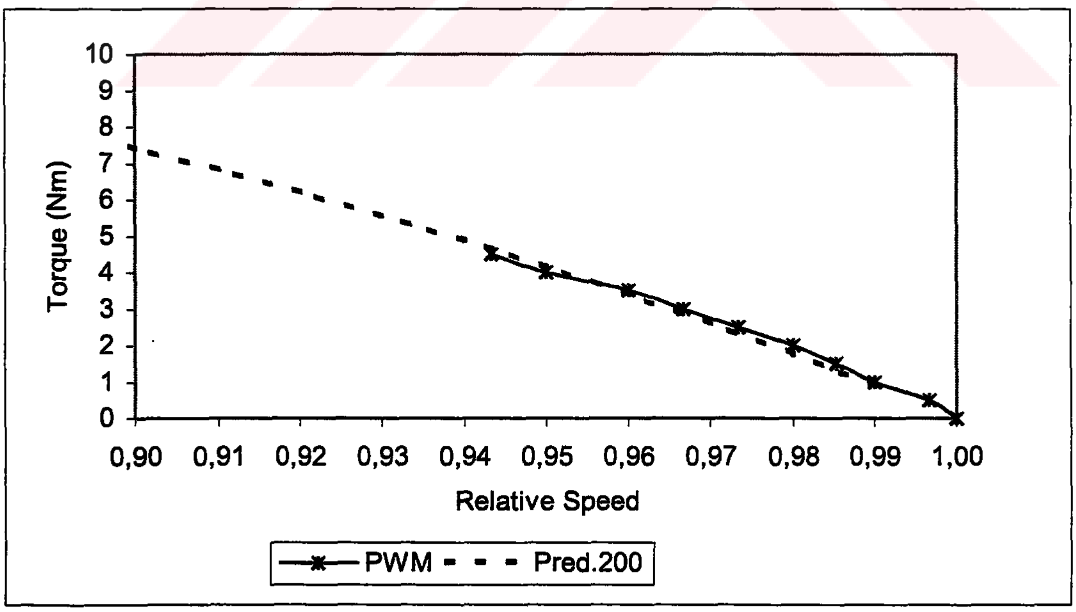

Figure A.V.2 Torque/speed curve for predicted pure AC at 200 Volt and PWM, f=50 Hz

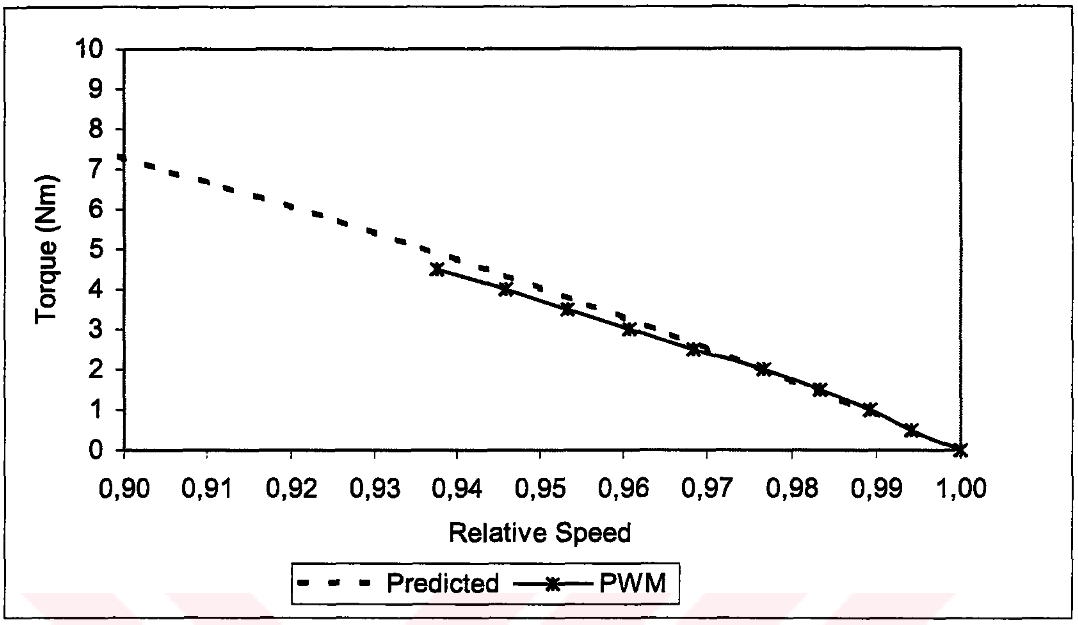

Figure A.V.3 Torque/speed curve for predicted and PWM test f=40 Hz

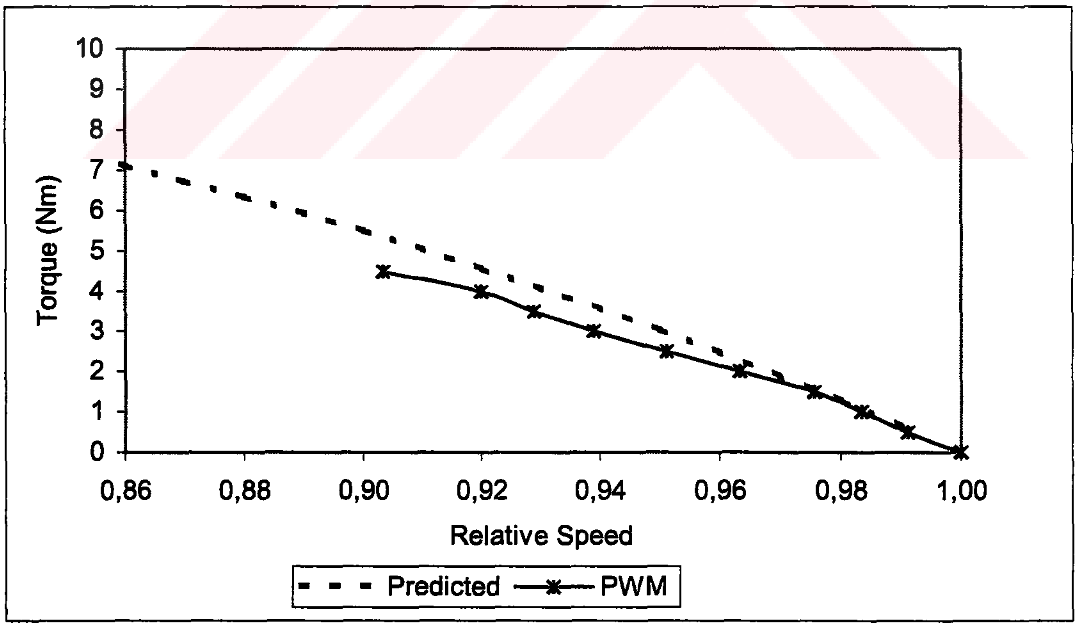

Figure A.V.4 Torque/speed curve f=30 Hz

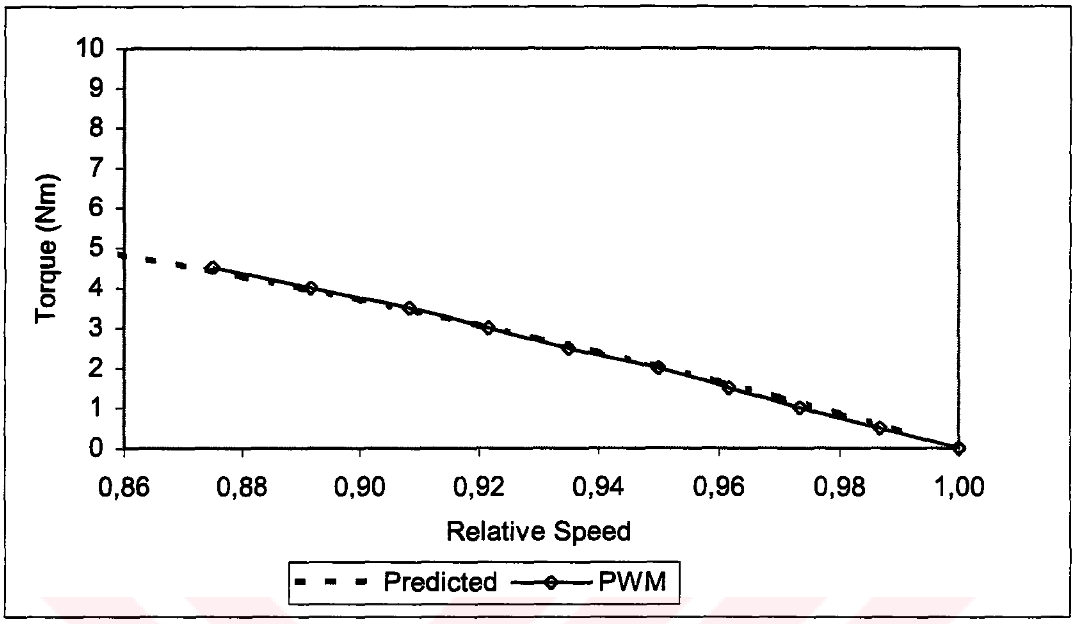

Figure A.V.5 Torque/speed curve f=20 Hz

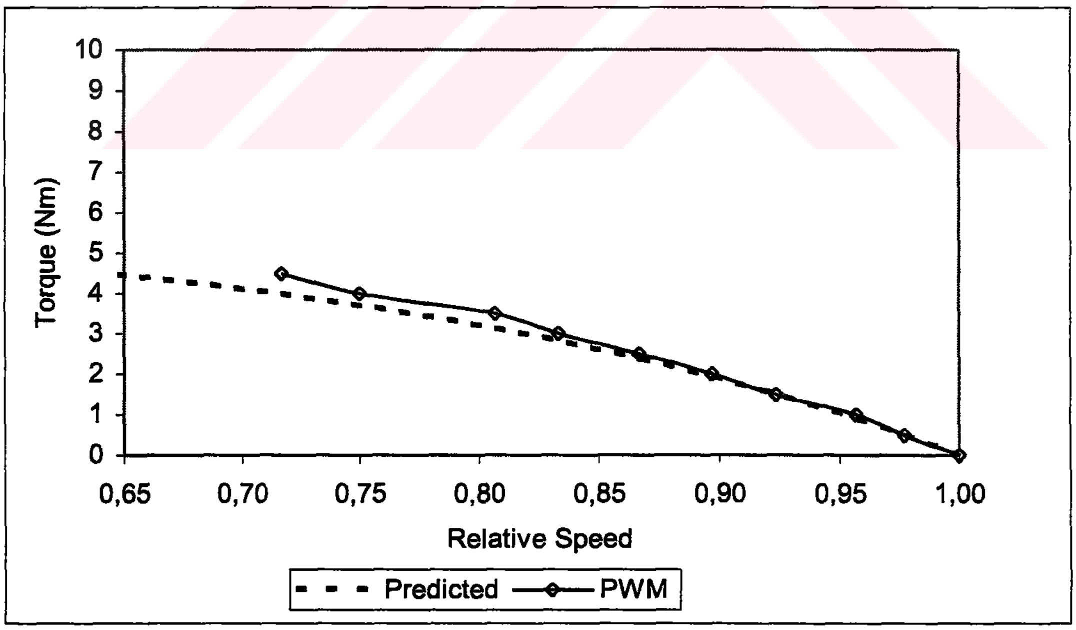

Figure A.V.6 Torque/speed curve f=10 Hz

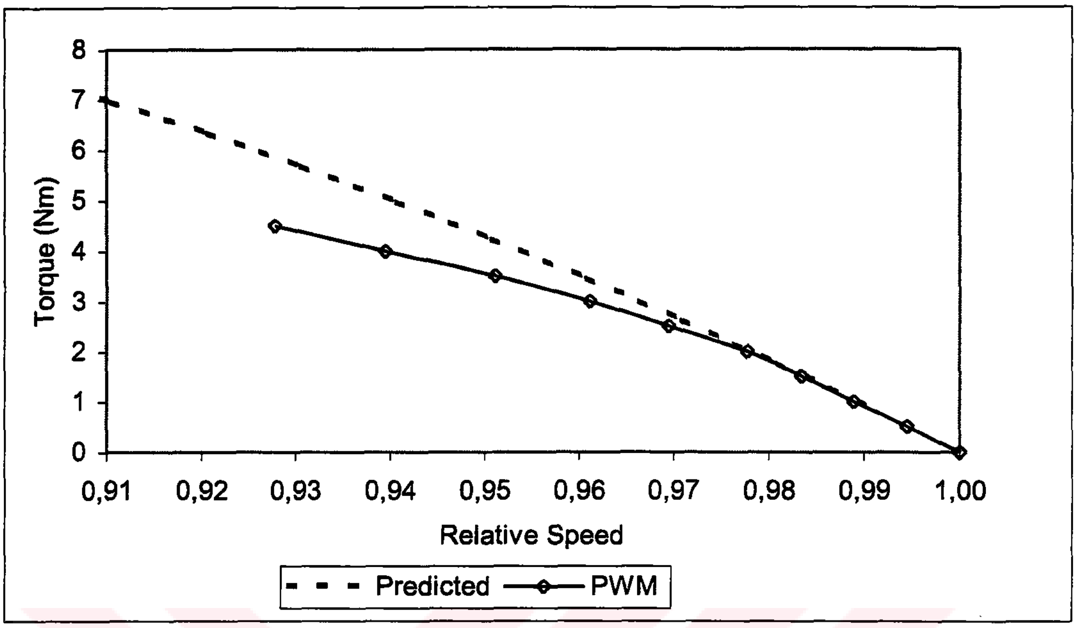

Figure A.V.7 Torque/speed curve f=60 Hz

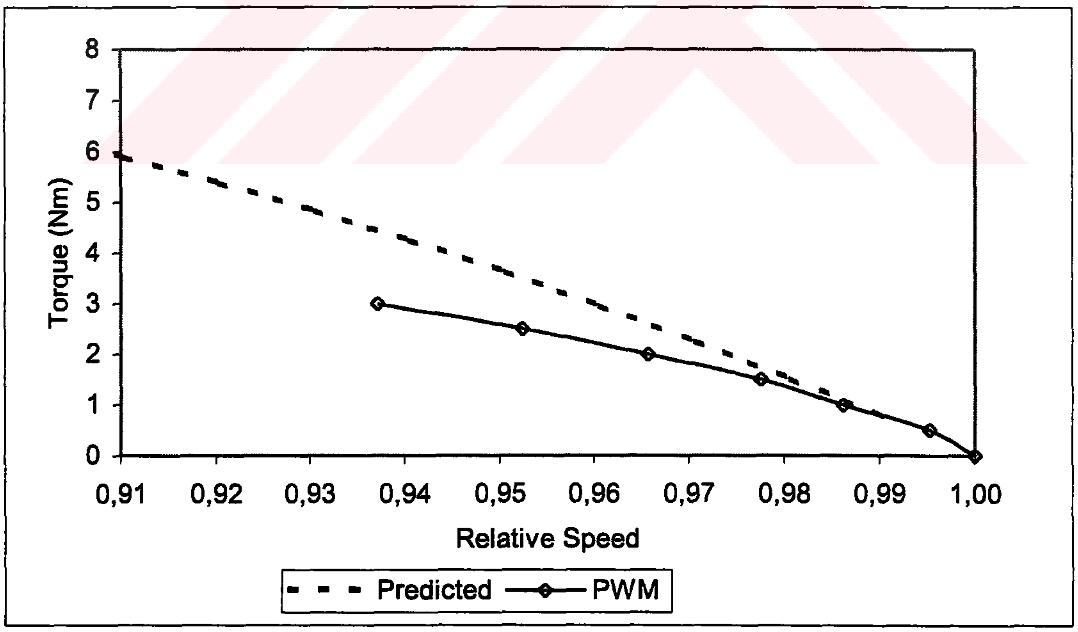

Figure A.V.8 Torque/speed curve f=70 Hz

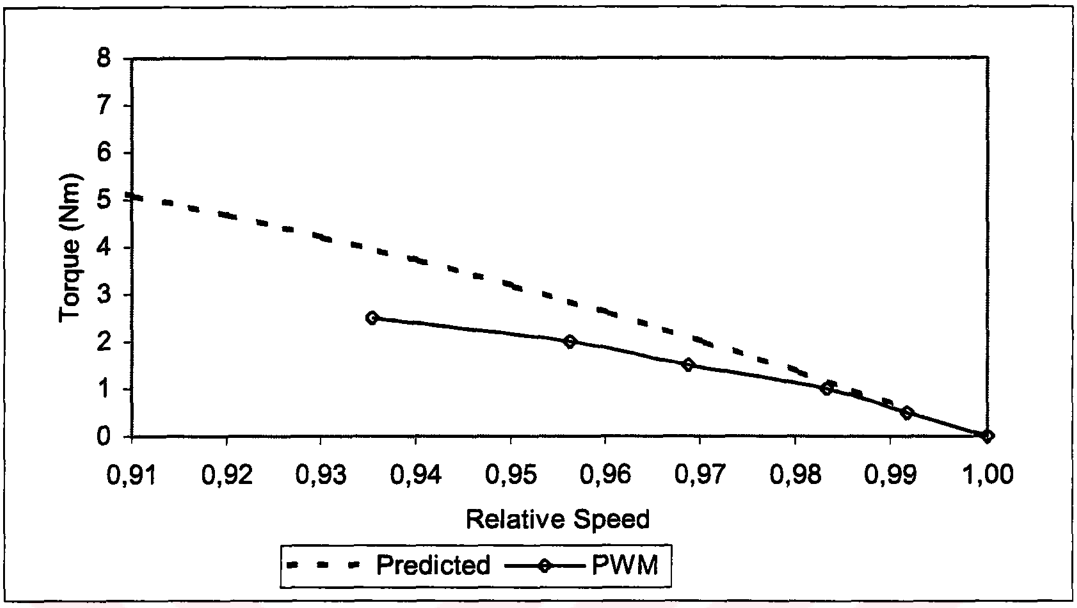

Figure A.V.9 Torque/speed curve f=80 Hz

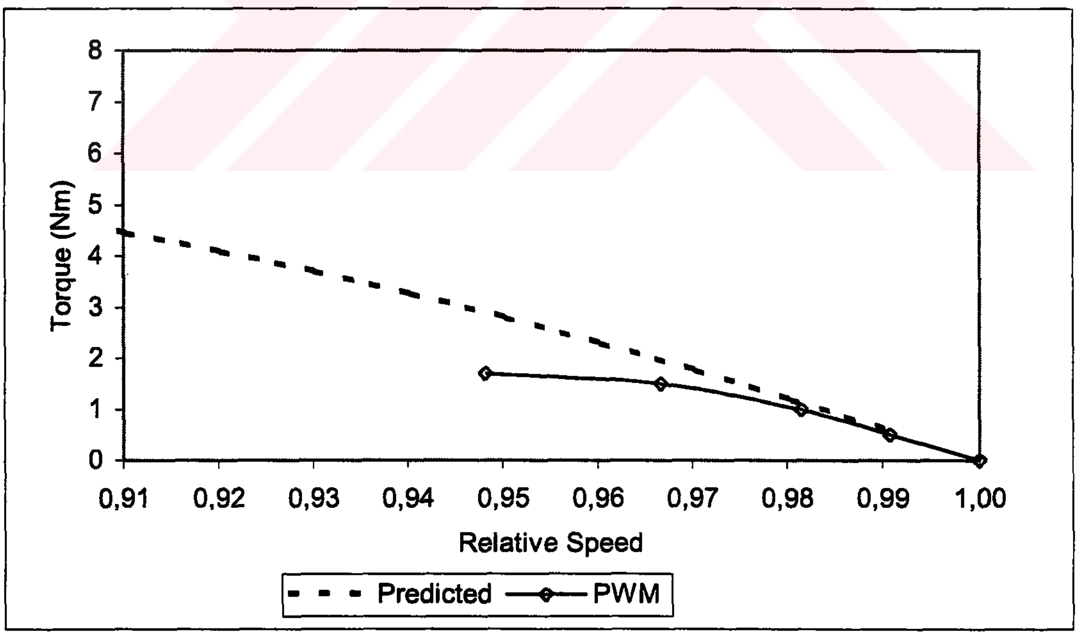

Figure A.V.10 Torque/speed curve f=90 Hz

A.VI. Harmonic Contents

Output waveform of Sinusoidal PWM inverter is shown in figure A.VI.1. In the figure, half-cycle output is shown with quarter wave symmetry and it is considered that notches are created on the square wave at predetermined four angles.

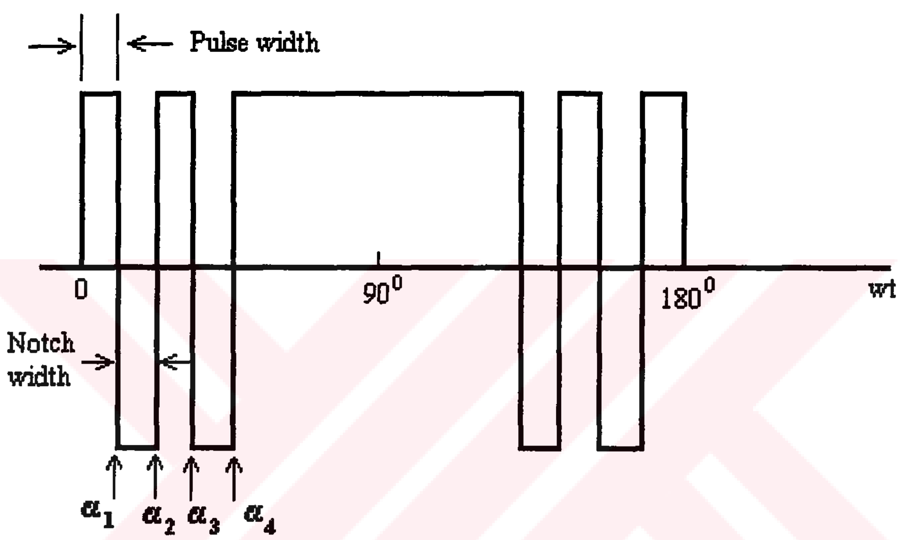

Figure A.VI.1 Output voltage waveform of Sinusoidal PWM inverter

The general Fourier series of the wave can be given as

$$v(t) = \sum_{n=1}^{\infty} (a_n \cos nwt + b_n \sin nwt) \qquad \text{A.VI.1}$$

where

$$a_n = \frac{1}{\pi}\int_0^{2\pi} v(t) \cos nwt \, dwt$$

$$b_n = \frac{1}{\pi}\int_0^{2\pi} v(t) \sin nwt \, dwt$$

For a waveform with quarter-cycle symmetry, only the odd harmonics with sine components will exits. Therefore coefficients are given as

$$a_n = 0 \qquad \text{A.VI.2}$$

$$b_n = \frac{4}{\pi}\int_0^{\pi/2} v(t)\sin nwt\, dwt \qquad \text{A.VI.3}$$

Assuming that the wave has unit amplitude i.e. $v(t) = \pm 1$, b_n can be expended as

$$bn = \frac{4}{\pi}\left[\int_0^{\alpha_1}(+1)\sin nwt\, dwt \;+\; \int_{\alpha_1}^{\alpha_2}(-1)\sin nwt\, dwt \;+\; \int_{\alpha_2}^{\alpha_3}(+1)\sin nwt\, dwt\right.$$

$$\left. + \ldots\ldots + \int_{\alpha_{i-1}}^{\alpha_i}(-1)^{i-1}\sin nwt\, dwt \;+\; \int_{\alpha_i}^{\pi/2}(+1)\sin nwt\, dwt\right] \qquad \text{A.VI.4}$$

Using the relation

$$\int_{\theta_1}^{\theta_2}\sin nwt\, dwt = \frac{1}{n}\left(\cos n\theta_1 - \cos n\theta_2\right)$$

the first and last terms are

$$\int_0^{\alpha_1}(+1)\sin nwt\, dwt = \frac{1}{n}\left(1 - \cos n\alpha_1\right) \qquad \text{A.VI.5}$$

$$\int_{\alpha_i}^{\pi/2}(+1)\sin nwt\, dwt = \frac{1}{n}\cos n\alpha_i \qquad \text{A.VI.6}$$

Integrating the other components of equation A.VI.4 and substituting equations A.VI.5 and A.VI.6 in it yields

$$b_n = \frac{4}{n\pi}\left[1 + 2\left(-\cos n\alpha_1 + \cos n\alpha_2 - \ldots\ldots + \cos n\alpha_i\right)\right]$$

$$= \frac{4}{n\pi}\left\{1 + 2\sum_{i=1}^{k}(-1)^i \cos(n\alpha_i)\right\} \qquad \text{A.VI.7}$$

A.VII. Multi-Level Converter

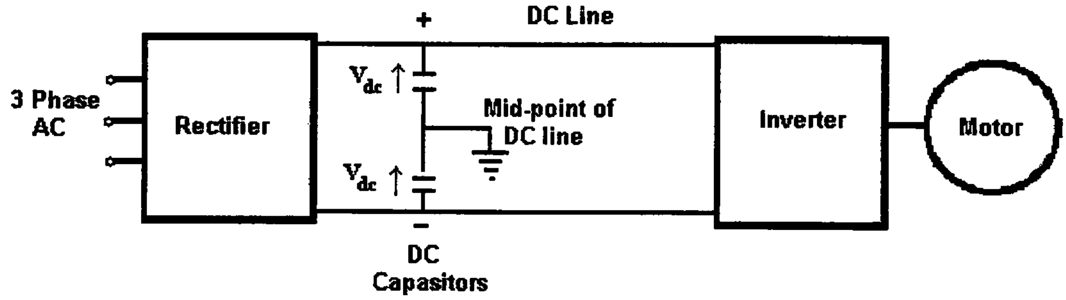

Figure A.VII.1 AC Drive Block Diagram

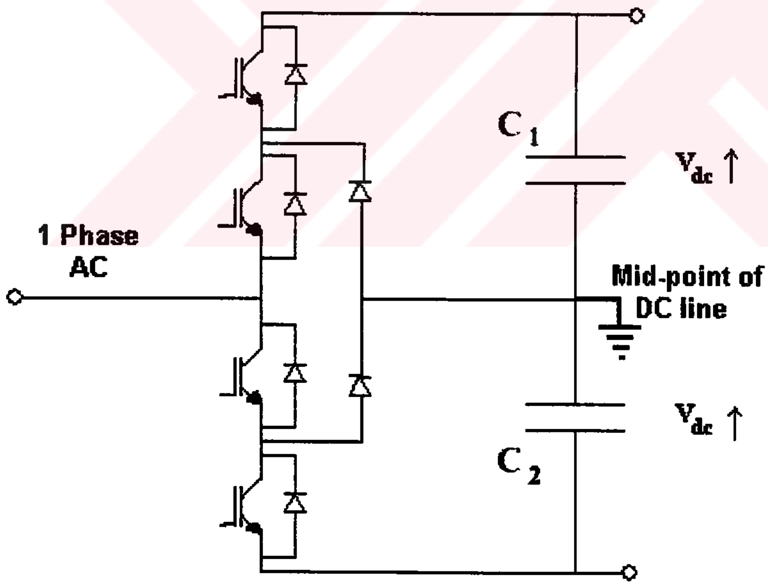

Figure A.VII.2 One Phase Circuit Diagram of Three-level Converter